Assessing the Hydrological Impact of Gravity-Fed Irrigation on Groundwater Recharge Using Long-Term Isotope Monitoring and Modelling

Vincent Marc, Franck Tison, Claude Doussan, Julien Dupont, Milanka Babic, Roland Simler, Stéphane Ruy

Hydrological Processes

WILEY

RESEARCH ARTICLE OPEN ACCESS

Assessing the Hydrological Impact of Gravity-Fed Irrigation on Groundwater Recharge Using Long-Term Isotope Monitoring and Modelling

Vincent Marc | Franck Tison | Claude Doussan | Julien Dupont | Milanka Babic | Roland Simler | Stéphane Ruy

Avignon Université, INRAE, UMR EMMAH, Avignon, France

Correspondence: Vincent Marc (vincent.marc@univ-avignon.fr)

Received: 3 January 2024 | **Revised:** 20 November 2024 | **Accepted:** 20 November 2024

Funding: The authors received no specific funding for this work.

ABSTRACT

This study investigates the hydrological processes driving groundwater recharge in the Avignon Plain (south-eastern France) through a detailed analysis of the interactions between irrigation, rainfall and soil water using long-term isotopic monitoring and lumped parameter modelling. More than 15 years of monthly isotopic data from rainwater, surface water, soil water and groundwater were analysed to quantify the contributions of gravity-fed irrigation and natural rainfall to aquifer recharge. Our results show that gravity-fed irrigation contributes about 85% of the recharge, highlighting the significant role of traditional agricultural practices in maintaining groundwater levels. Through isotopic tracing and modelling, we observed variations in transit times, with faster infiltration pathways associated with irrigation flows compared to more prolonged recharge from rainfall. This study not only demonstrates the effectiveness of isotopic techniques for assessing water sources in complex recharge scenarios but also provides insights into how irrigation practices affect groundwater sustainability. These results contribute to current thinking on sustainable water management and highlight the need for integrated approaches that reconcile agricultural water use efficiency and groundwater conservation.

1 | Introduction

Since the middle Ages, river channelling has been common in the northern Mediterranean regions, primarily to supply hydraulic power to mills for processing wheat, hemp, paper, oil and other products (Aspe 2012; Livet 1980). At that time, irrigation water mainly came from runoff collected in terrace-like structures and local populations cultivated crops suited to the climate, such as vineyards, olive trees, cereals, and legumes (Aspe 2012). Following the French Revolution, the rapid growth of agricultural society led to a significant increase in irrigation practices, peaking in the 19th century. During this period, gravity-fed irrigation – diverting water from rivers to flood fields – became widespread. Water was conveyed from surface sources, primarily rivers or reservoirs, and distributed to fields through a network of canals or pipelines using gravity. At the early 2000s, this irrigation method still accounted for 40% of the total irrigable area in Languedoc and Provence, utilising 80% of the total withdrawn water volume (AIRMF 2009). While not highly water-efficient, these practices provide indirect benefits, such as recharging shallow groundwater, often used for drinking water supply (Kuhfuss and Loubier 2013; Masseroni et al. 2017; Nofal et al. 2019; Bouimouass et al. 2022). Climate change models indicate that Mediterranean regions are likely to experience increasingly frequent and severe droughts, as well as intense rainfall events causing high runoff (Tebaldi et al. 2006; Lorenzo and Alvarez 2022). To address these issues, innovative methods of annual water management are essential for capturing excess water and storing it in aquifers protected from evaporation. Induced infiltration, achieved through the use of dry wells or soakaway ponds, can be one solution (Edwards et al. 2016;

Sasidharan et al. 2021). Some authors suggest using agricultural infrastructure, especially canal networks, for artificial recharge of the aquifer (Niswonger et al. 2017). Managed aquifer recharge (MAR), which involves the artificial infiltration to aquifers, has long been proposed as a solution for regions with pronounced seasonal climate (Bredehoeft, Papadopulos, and Cooper Jr 1982; Bouwer 2000; Dillon et al. 2010). The artificial recharge of aquifers in agricultural areas has been successfully implemented in several regions (Niswonger et al. 2017; Godwin et al. 2022; Ali et al. 2023). This approach offers a significant over traditional methods, such as wells and infiltration basins, by providing larger infiltration areas. This is facilitated by the proximity of the hydrographic network and the availability of hydraulic infrastructures for irrigation, such as networks of canals and ditches.

A variety of methods have been used to analyse the impact of recharge processes on aquifers (Scanlon, Healy, and Cook 2002; Healy 2010; Felfelani et al. 2024). Some techniques focus on infiltration estimates or soil drainage, while others approach recharge analysis based on groundwater data. The first group of methods includes measuring infiltration rates using lysimeters (Stumpp, Maloszewski, et al. 2009; Stumpp, Stichler, and Maloszewski 2009; Reszler and Fank 2016; Sobaga et al. 2024), isotopes tracers (Koeniger et al. 2016; Tao et al. 2021), infiltration process modelling (Gogolev 2002; Ganot et al. 2017; Gong et al. 2023), the use of artificial tracers like Br^- or brilliant blue (Nobles, Wilding, and Lin 2010; Zhang et al. 2017; Chen et al. 2021), geophysical measurements (Cook et al. 1992; Maliva, Clayton, and Missimer 2009) and empirical techniques, such as the empirical weight function method which assumes that groundwater recharge can be expressed through a Poisson probability density function (Jie et al. 2022; Zhang et al. 2024). Most of these methods are local in scope and require integration with spatial approaches for broader applications. The second group of techniques include piezometric monitoring and water budget calculations (Lacroix, Wang, and Blavoux 1996; Racz et al. 2012; Cuthbert et al. 2016), the chloride mass balance method (Gee et al. 2005; Ifediegwu 2020) and environmental tracers (Cartwright et al. 2017; Séraphin, Vallet-Coulomb, and Gonçalvès 2016; Bouimouass et al. 2020; Chmielarski et al. 2024). A key advantage of methods using groundwater data is that they directly estimate recharge rates rather than only infiltration or drainage. Among these, environmental tracing techniques are especially valuable as they assess average recharge over several square kilometres, addressing the spatial variability in recharge. Commonly used radioisotopes include ^{3}H, ^{14}C and ^{36}Cl, selected according to the expected average residence time in the aquifer under study (Blavoux et al. 2013; Müller et al. 2016; Batlle-Aguilar et al. 2017; Zouari et al. 2024) as well as noble gases radioisotopes like ^{39}Ar, ^{81}Kr and ^{85}Kr (Gerber et al. 2017; Mayer et al. 2014). Short-residence-time atmospheric contaminants, such as CFCs and SF_6 (Bartyzel and Rozanski 2016) or short-lived natural radionuclides (Schubert et al. 2024) are also useful for evaluating recent recharge processes. Another important group of tracers includes the stable isotopes of water, ^{18}O and ^{2}H. These isotopes are cost-effective, enabling routine monitoring, and recent advances of laser optical measurement technology now allow for the rapid collection of large quantities of ^{18}O and ^{2}H data directly in the field (Tweed et al. 2016; Kühnhammer et al. 2022). With these extended time-series data on both input sources (rain, irrigation, etc.) and outputs (outlet, spring, well, etc.), transfer times and the tracer concentrations can be analysed using lumped parameters models (LPM) (Maloszewski and Zuber 1996). LPMs are frequently applied to model isotopic variations in soil water (Maloszewski et al. 2006; Stumpp, Maloszewski, et al. 2009; Stumpp, Stichler, and Maloszewski 2009; van Wyk, Dippenaar, and Ubomba-Jaswa 2024) and groundwater (Małoszewski and Zuber 1982; Maloszewski et al. 1992; Blavoux et al. 2013; Musgrove, Jurgens, and Opsahl 2023; Gourdol et al. 2024; Li et al. 2024) across various hydroclimatic conditions. Typically, these models use a single transfer function to represent the distribution of transfer times in a presumed homogeneous medium. Moreover, LPMs applied in aquifer studies (e.g., wells or piezometers sampling) often focus on groundwater–river interactions (Fórizs et al. 2005; Kármán et al. 2014; Le Duy et al. 2019).

- In this study, we utilise a long-term isotopic record of rainwater, soil water, groundwater and irrigation water to propose a time-dependent analysis of groundwater recharge conditions under gravity-fed irrigation practices. We aim to analyse soil infiltration dynamics and transit time distribution in groundwater through a combination of isotopic transfer models. This analysis provides a comprehensive view of recharge processes, highlighting the temporal contributions of different water sources and estimating variations in transfer times based on recharge patterns. Specifically, we will explore the following questions:
- What is the quantitative contribution of gravity-fed irrigation to the recharge of the shallow alluvial aquifer in the Avignon region, and how does it compare with natural rainfall recharge?
- How do infiltration processes differ between rainwater and irrigation water, and what are their respective transit times in the soil and aquifer as indicated by isotopic analysis?
- To what extent can lumped parameter models accurately simulate the isotopic variability in groundwater under the dual influence of rainfall and irrigation, and what improvements can be suggested for better capturing recharge dynamics?

2 | Study Area and Methodology

2.1 | Historical and Regional Context of Irrigation Practices

The earliest hydraulic installations that transported water from the Durance River to the plains near Avignon, France, date back to the 13th century. Over time, local farmers organised to establish irrigation systems, eventually forming water unions – association of landowners – by the early 20th century. The alluvial plain downstream of the Durance River, extending to its confluence with Rhône River, has since undergone significant changes, notably a decrease in the number of farmers and an increase in

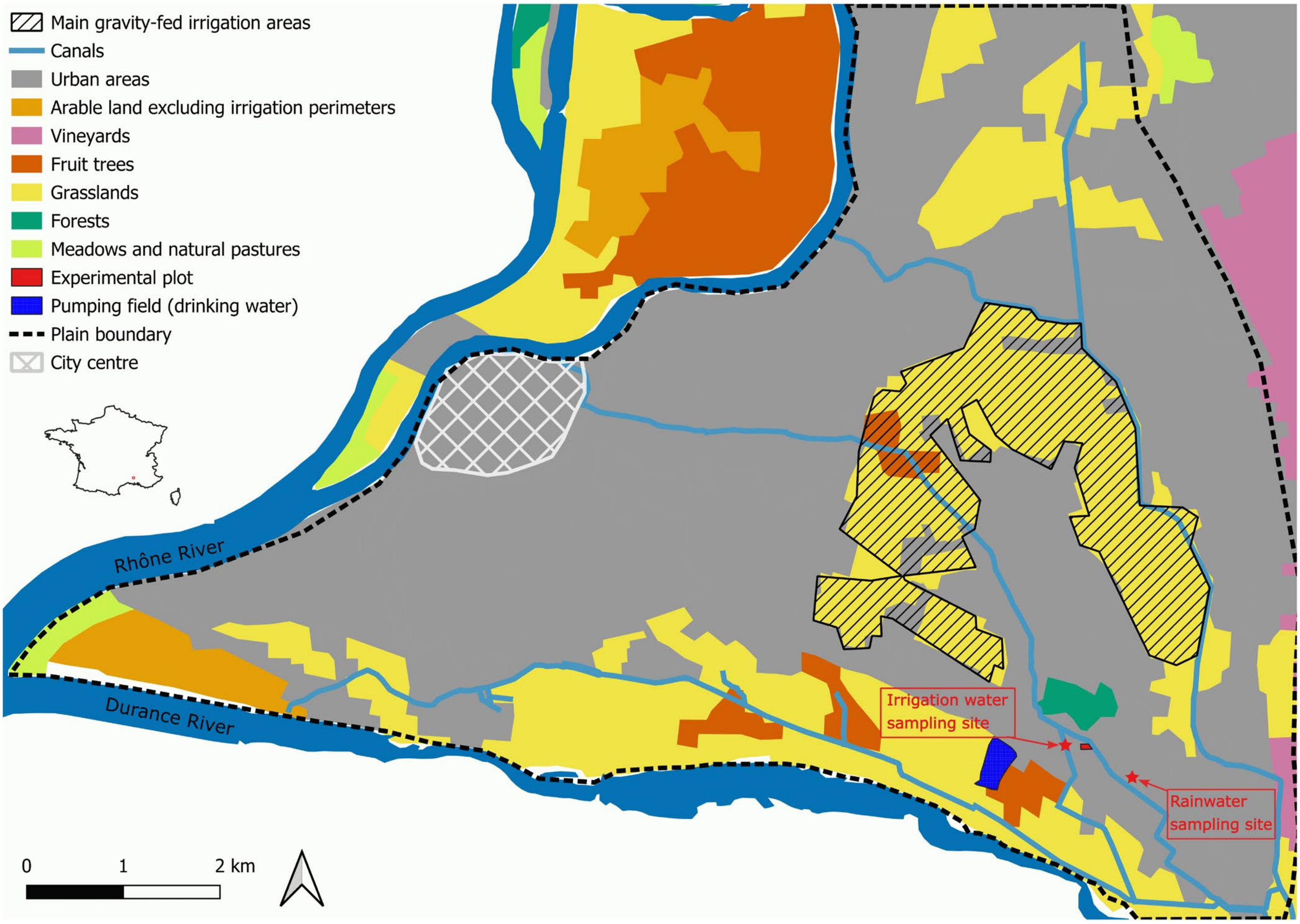

FIGURE 1 | General location of the Avignon alluvial plain and the study area.

urbanisation. Today, the canal network in the plain is managed by an authorised association of syndicates (ASA) which oversees irrigation for the Avignon plains (Figure 1). Water is drawn from a main canal connected to the Durance River, just southeast of the plain's boundary.

2.2 | Study Site Description and Data Collection Techniques

The study area is located in the upstream section of the Avignon alluvial aquifer, approximately 1 km north of the Durance River (https://www.canaux-avignon.fr/; Figures 1 and 2). This aquifer is bordered by the Durance River to the south, the Rhône River to the east, and north–south oriented relief formed by colluvium, silt and marl to the west. It consists of quaternary alluvial deposits – a mixture of pebbles, gravel, sand and silt – with a thickness of 10–15 m (Figure 2). The uppermost layer comprises silt which progressively thickens from east to west. Towards the western edge, these silts become increasingly clay-rich, forming a confining unit above the aquifer. Beneath this lies bedrock composed of burgigalian blue marl. The piezometric map shows that groundwater flows from east to west, with a relatively steady hydraulic gradient, except in upgradient areas to the east, where runoff occurs along the slopes. The experimental area is potentially influenced by the Durance River but is mainly affected by the recharge from upstream irrigated zones (Lacroix, Wang, and Blavoux 1996; Nofal et al. 2019). The alluvial plain contains a substantial proportion of urbanised areas, particularly in the western part, on the banks of the Rhône, where Avignon's city centre is situated (Figure 1). Urbanisation is also expanding eastwards, with the development of satellite villages and commercial areas. The Durance River forms the eastern boundary of the plain, where the agricultural land is largely made of hay meadows, fruit orchards and vineyards. Gravity-fed irrigation is the primary irrigation method used for these meadows and in the central eastern part of the plain. However, this irrigation technique is not applied in the immediate vicinity of the experimental plot, as the nearest irrigated fields upstream are located at least 1 km to the northeast (Figure 1). The alluvial aquifer supplies drinking water to approximately 100 000 people, with an average daily pumping volume of 35 000 m^3/day, reaching up to 50 000 m^3/day during the summer months (Nofal et al. 2010).

The 0.6-ha experimental plot is equipped with 14 pairs of piezometers installed at a relatively shallow depths (reaching the water table fluctuation zone, around 8 m deep) and deeper depth (reaching bedrock, around 15 m deep) to monitor the water table at the interface with the unsaturated zone and across its full thickness. These piezometers are fitted with 64/75 mm PVC pipes and are screened over 2 or 5 m, depending on the borehole depth. A 2/4 mm gravel pack is placed around the screened section, while the solid portion of the

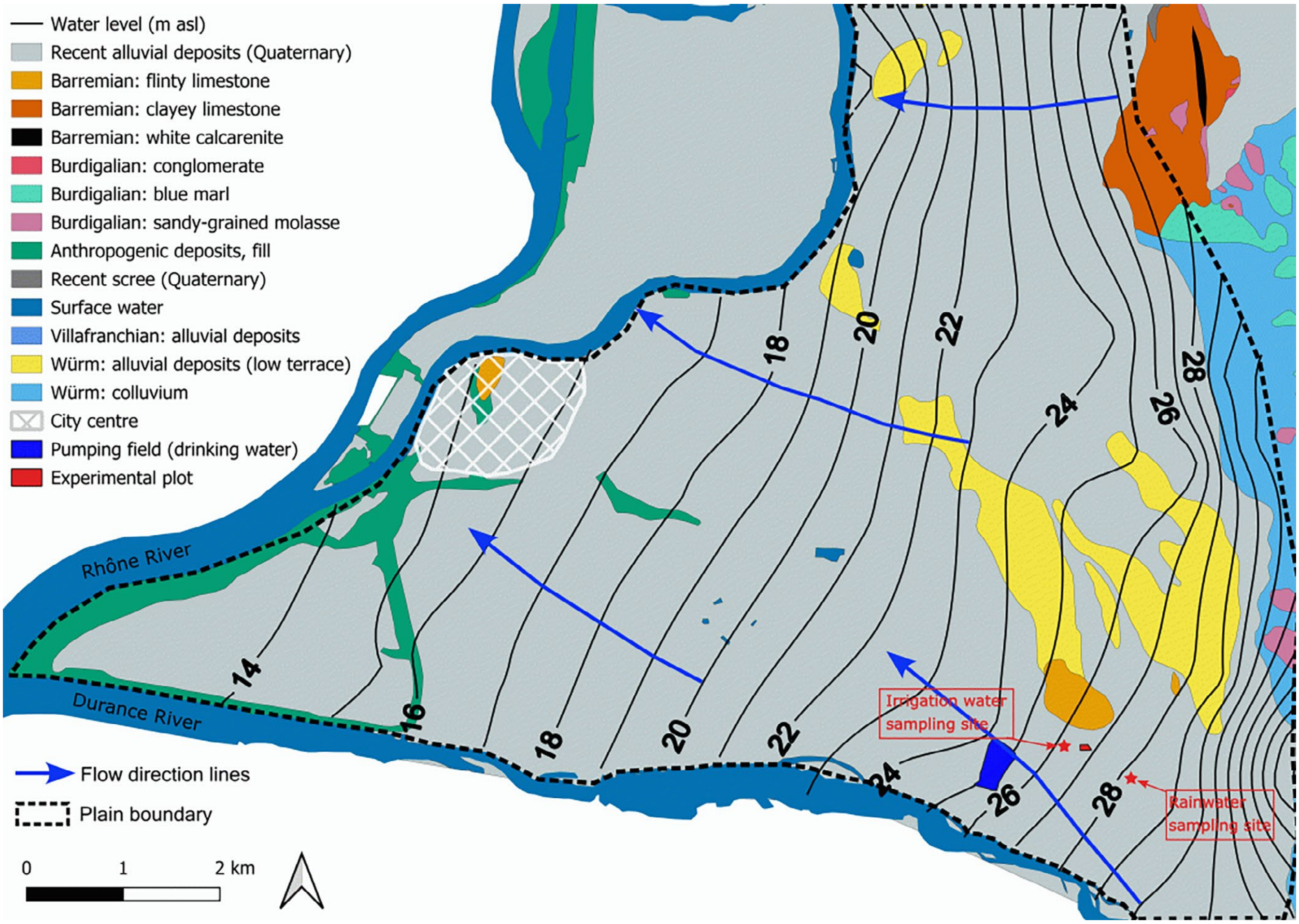

FIGURE 2 | Main geological settings and general piezometric map (after Nofal et al. 2019).

TABLE 1 | List of suction lysimeters for soil water sampling at different depths.

Site A		Site C	
Name	**Depth (cm)**	**Name**	**Depth (cm)**
BPA1	19	BPC1	16
BPA2	28	BPC2	26
BPA3	50	BPC3	49
BPA4	98	BPC4	101
BPA5	200	BPC5	179

pipe is sealed with a watertight sobranite plug. The boreholes are sealed with a cement grout and a metal protective tube, fitted with a cap at the head and a base plug. In addition, two locations are designated for soil water content measurement (Table 1 and Figure 3). The soil at the experimental site is a deep calcisol (1.6–2.5 m deep), consisting of silty clay (0–90), clay loam (90–180 cm) and sandy loam (180–240 cm) (Bogner et al. 2013; Brillard et al. 2015). The surface clay layer is well-structured, developing a network of cracks during summer desiccation. These cracks can reach widths of approximately 1 cm and depth of 40 cm. Groundwater from two selected piezometers (8 and 12, see Figure 3) has been sampled monthly for isotopic analysis since 2007. These piezometers are screened throughout the full thickness of the water-table aquifer. Sampling was carried out using an electric pump at a rate of 3 L/min for 15-min to ensure complete renewal of the water column. Concurrently, water was sampled from neighbouring nearby irrigation canal, along with soil water at various depths (16–200 cm, Table 1), using suction lysimeters (monitoring started in 2004). The water from the lysimeters was collected after 24 h of pressure depression. Isotopic analyses were performed on both groundwater and soil water samples. Additionally, the monthly isotopic content of rainfall was obtained from Avignon University's collection station, which is part of the GNIP (global network for isotopes in precipitation) and the Renoir network (French National Observatory Service https://sno-renoir.osups.universite-paris-saclay.fr/). This station, located 600 m southeast of the plot, has been collecting data since August 1999. Rainfall samples are gathered from each event and stored in an airtight container in a cool, dark place to provide a monthly composite sample. Prior to analysis, the water can be stored in 20 mL brown glass bottles briefly under cool, dark conditions. Isotopic analyses are conducted at Avignon University using a cavity ringdown spectrometer (L2140-I Picarro). For each sample, six measurements are taken, with only the final three used to calculate results. The analytical uncertainty, based on 2 times the standard deviation of these last three measurements is approximately 0.1‰.

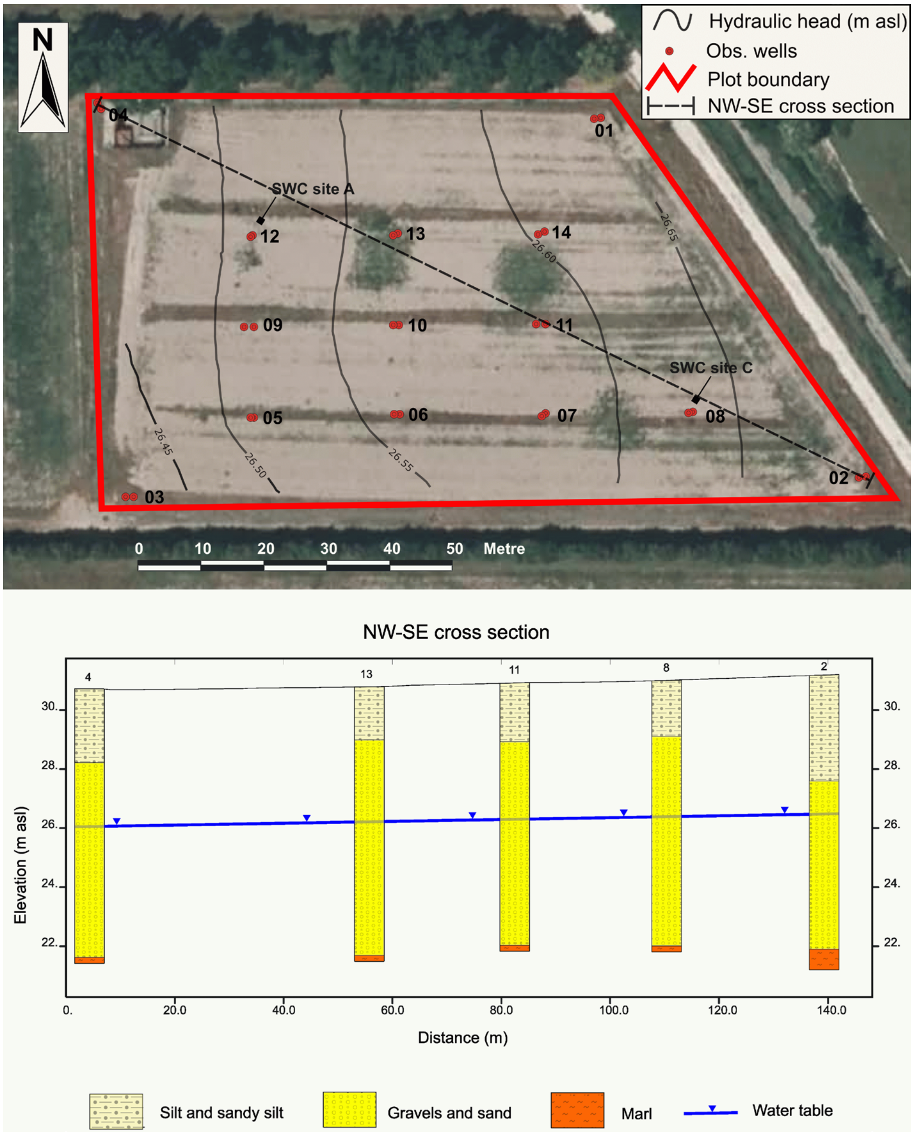

FIGURE 3 | Experimental plot – hydrogeological context and position of soil water sampling sites.

In terms of hydrogeology, automatic TD Diver pressure sensors (accuracy ±0.5 cm) are installed in four piezometers at the corners of the plot (1, 2, 3, 4), with all points also subject to a monthly manual piezometric survey.

2.3 | Modelling Framework for Recharge Processes

We conducted monthly isotope simulations of soil water and groundwater under the assumption that the monthly water and isotope rates were in a pseudo-steady-state, represented by:

$$Q_{out} = Q_{in} {}^{*} g(T) \text{ and } F_{out} = F_{in} {}^{*} g(T)$$

where Q_{out} et Q_{in} are the outgoing and incoming water rates respectively, F_{out} et F_{in}, are the outgoing and incoming isotopic rates ($Q \times \delta$) respectively, $g(T)$ is the transfer function dependent on the mean transit time T and * denotes the convolution operator.

The resulting isotopic content was calculated by taking the ratio of F_{out} to Q_{out}. The function $g(T)$ characterises the mixing behaviour across different time fractions and several transfer functions were tested to evaluate this mixing. In the functions below, t represents the sampling time and t' the time at which the water particle entered the system:

- Piston flow model, PFM: Represents direct transfer from the inlet (recharge area) and the system outlet (lysimeter or piezometer) without dispersion or mixing:

$$\mathrm{PFM}_{g(t-t')} = \delta\left(t - t' - T\right)$$

- Exponential mixing model, EMM: Assumes a transit time distribution from 0 to infinity, where the shape depends solely on T (Jurgens et al. 2012).

$$\mathrm{EMM}_{g(t-t')} = \frac{1}{T} e^{\left(-\frac{t-t'}{T}\right)}$$

- Exponential – piston-flow model, EPM: Combines the complete mixing EMM model and the no-mix transfer model PFM (Jurgens et al. 2012)

$$\mathrm{EPM}_{g(t-t')} = \frac{n}{T} e^{\left(-\frac{n\left(t-t'\right)}{T}+n-1\right)} \qquad \text{for } t > (n-1)T/n$$
$$\mathrm{EPM}_{g(t-t')} = 0 \qquad \text{for } t <= (n-1)T/n$$

With n, the ratio between the total volume of the aquifer and the volume concerned by the exponential transfer.

- Dispersive model, DM: Uses a transit time distribution dependent on a dispersion coefficient (related to the average distance from the recharge to sampling zones and the medium's dispersivity). This approach assumes that the tracer is introduced and sampled in proportion to the rate in a semi-infinite medium, suitable for instantaneous injection and detection (CFF mode) in our aquifer configuration (Małoszewski and Zuber 1982):

$$DM_{g(t-t')} = \frac{1}{T}\frac{1}{\sqrt{4\pi DP\frac{t-t'}{T}}} e^{\left(-\frac{\left(1-\frac{t-t'}{T}\right)^2}{4DP\frac{t-t'}{T}}\right)}$$

With DP is the dispersion parameter: $DP = \frac{D}{vx}$, where D is the dispersion coefficient, v is the velocity and x is the outlet position.

We also examined several transfer configurations:

- A single transfer system using a selected transfer function

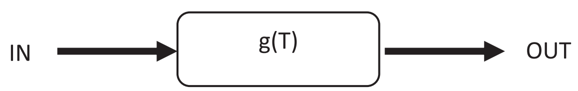

- A binary transfer system with 2 flow paths (e.g., matrix flow and preferential flow) where p represents the proportion of flow through path 1:

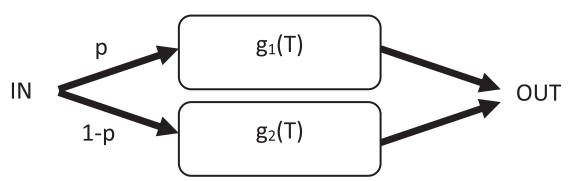

The soil input function was based exclusively on monthly rainfall data, while the groundwater input function included both rainfall and irrigation rates. Initially, we assumed the alluvial groundwater received recharge across its entire surface area (Figure 4a), with the EMM model deemed suitable for simulating transit times distribution. However, the surface is underlain by a silt layer that thickens downgradient, creating a confining effect on the water table in certain areas (Figure 4b). This scenario could be better simulated using an EPM or DM model. These configurations are also suitable for situations when recharge zone is distant from the sampling point, as is the case for irrigation-sourced recharge in this study.

Our modelling approach was consistent for both groundwater and soil water, applying several transfer functions independently, such as the exponential and dispersive models. Additionally, we tested binary models different configurations: DM-PFM, DM-EMM, DM-EPM and DM-DM.

Model parameters (T, DP, n) were calibrated by minimising the discrepancy between simulated and observed data, with two optimisation metrics used were RMSE and KGE:

Root mean square error (RMSE):

$$\mathrm{RMSE} = \sqrt{\frac{\sum_{i=1}^{n}\left(y_i - y_{\mathrm{sim}-i}\right)^2}{n}}$$

where n is the sample size, i is the range of the sample point, y_i is the ith observation value and $y_{\text{sim-i}}$ is the ith simulated value.

Kling Gupta Efficiency (KGE) (Gupta et al. 2009): $1 - \sqrt{(r-1)^2 - (\alpha-1)^2 - (\beta-1)^2}$. where r is the correlation coefficient, α is the bias ratio (ratio of observed and calculated averages) and β is the variability ratio (ratio of observed and calculated standard deviations).

A multi-criteria evaluation framework is often recommended to assess diverse model aspects, enhancing the robustness of result interpretation (Jackson et al. 2019; Clark et al. 2021; Cinkus et al. 2023). RMSE provides the mean absolute deviation from the measurements and is widely used to optimise LPMs, typically alongside a correlation criterion (coefficient of determination) and a criterion for model over- or underestimation (Stumpp, Maloszewski, et al. 2009; Stumpp, Stichler, and Maloszewski et al. 2009; Eberts et al. 2012). We additionally used the KGE as a complement to the RMSE to evaluate the model's performance across bias, variability and correlation.

3 | Results and Hydrological Insights

3.1 | Estimating Irrigation and Rainfall Rates

There are currently no effective methods for accurately measuring the actual amount of irrigation water supplied to fields. Irrigation practices at the plot level rely on informal communication between upstream and downstream users, as well as with the water unions, remaining largely empirical. Users of an irrigation system select the days and duration of plot submersion based on the available water flow from the canal, which directly depends on the actions of the other users. Any surplus water in the primary canal is directed downstream towards either the Durance or Rhône rivers. Consequently, the daily amount of irrigation water reaching the plots varies significantly, influenced by factors unrelated to plant needs, such as user availability. Given these circumstances, accurately estimating the total volume of water supplied, even on a monthly

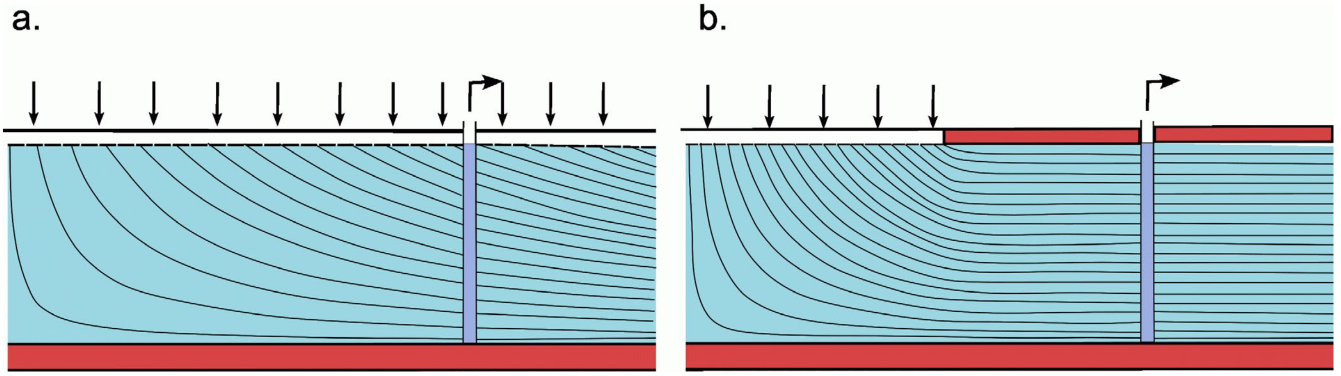

FIGURE 4 | Possible configurations of the system. (a) Recharge on the whole surface of the aquifer. (b) Recharge on a part of the aquifer from (Jurgens et al. 2012).

basis, is challenging. However, discharge at one branch of the canal network was measured at several points between March 2000 and August 2010, allowing a reasonably accurate estimation of the water volume distributed within the branch's area of influence. As preliminary estimate, water volumes per unit area were extrapolated to cover the entire plain (Nofal 2014). Due to maintenance and management costs, this monitoring only continued until 2010. A method was later proposed to estimate water volumes based on the relationship between the irrigation rate and the reference evapotranspiration, allowing for estimates from 2010 to 2021. The linear regression model produced a statistically significant fit ($r^2 = 0.87$), though prediction uncertainty remains high (Figure 5a). The model exhibits the greatest deviations in March and August, with offsetting effect across spring (underestimation) and summer (overestimation) (Figure 5b). Ultimately, a relative error of at least 20% was estimated for the monthly irrigation rates.

The time series of irrigation rates time series reveals a distinct seasonality pattern, with maximum supply levels exceeding 700 mm in August, and zero irrigation during the period from November to February (Figure 6a). The irrigation season typically begins in March and ends around mid-October, after which the canals are closed until the following spring.

Rainfall data were collected from the Meteo France climatic station 84 007 004, located 500 m from the experimental plot. The mean annual rainfall is 684 mm. The area experiences a wet autumn season with high rainfall totals and intensities, known as "Cevenol episodes", a similarly rainy spring with moderate rainfall, and two drier seasons in winter and summer. Heavy autumn rains can produce monthly totals rarely exceeding 200 mm, typically occurring 2 months after peak irrigation (Figure 6a).

3.2 | Hydrogeological Dynamics of the Alluvial Aquifer

Since January 2005, continuous monitoring of water levels in the aquifer has revealed a cyclical variation in hydraulic heads, corresponding with the seasonal pattern of irrigation (Figure 6b). The influence of irrigation on groundwater level fluctuations is evident from the strong correlation between these variables, unlike the relatively weak correlation observed between rainfall and groundwater levels (Figure 6c). The seasonal variation in water table levels ranges from 1 to1.5 m, with no substantial differences in dynamics among the piezometers. Additionally, there is no notable difference in water levels between the shallow and deep piezometers. However, a consistent difference in water levels was noted between points 2 and 3. Since these piezometers are aligned along the same flow line, the discrepancy reflects a localised head loss within the water table between upstream and downstream.

Furthermore, an upward trend of approximately 30 mm per year in water levels has been observed across all piezometers. This increase appears unrelated to the amount of irrigation water applied. Instead, it is more likely attributable to changes in flow conditions in the Durance River, following upstream modifications in 2006 that resulted in an increased flow.

3.3 | Isotopic Analysis of Water Sources

The isotopic time series for rainwater, irrigation, soil and groundwater at the site is displayed in Figure 7. The sequence started in March 2004 when the initial soil water samples (BPA4 and BPA5) became available.

Over 15 years of isotopic monitoring revealed that soil water closely resembled the rainwater signal, with a clear attenuation effect evident with increasing depth. The arithmetic mean values of the soil water isotopic signal at various depths were as follows (SD = 0.1‰): −6.37‰, −6.43‰, −6.38‰, −6.34‰ and −6.57‰ for BPA1, BPA2, BPA3, BPA4 and BPA5, respectively. The weighted average of $\delta^{18}O$ in gross rainfall was −6.40‰, with a standard error (SE) of 0.29‰, calculated following the method by Kirchner and Allen (2020). There were no significant differences in the isotopic content across soil water samples from various depths, and the average isotopic content of these samples was closely aligned with that of gross rainfall. These findings suggest that evaporation did not have a marked effect on soil water's isotopic values of soil water, and that the precipitation signal was largely preserved. This is further supported by an analysis of the $\delta^{18}O/\delta^{2}H$ relationship, which shows that all soil water points lie along the local meteoric water line (LMWL) (Figure 8).

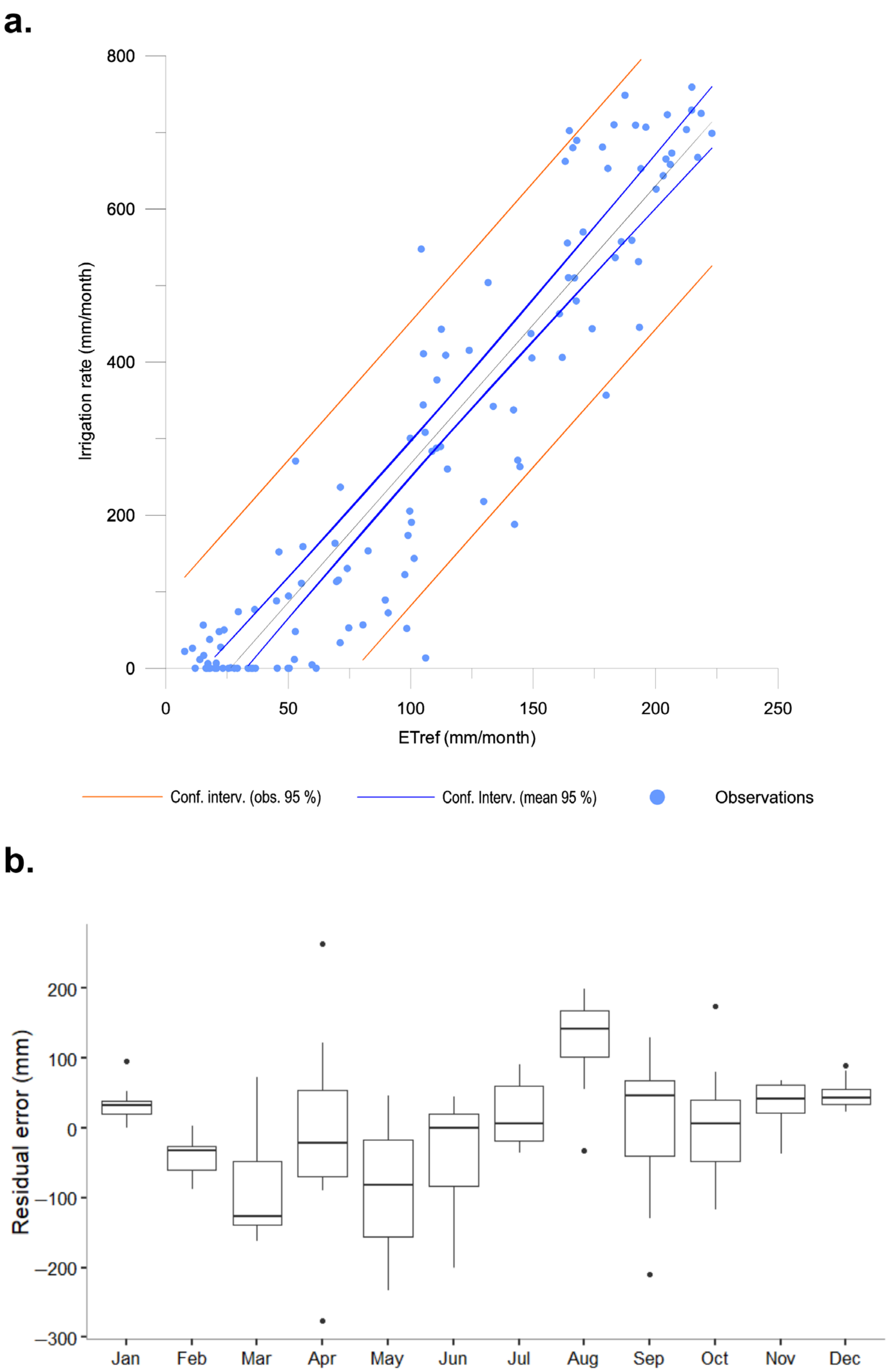

FIGURE 5 | (a) Correlation between monthly ETRef and measured irrigation rates (period March 2000–August 2010). (b) Residual error of the regression model (observed values-calculated values).

Groundwater samples from piezometers 8 and 12 showed no significant differences in isotopic values or behaviour. For further analysis, piezometer 12, with the most complete time series data, will be used. The isotope composition of the irrigation water substantially influenced the average isotopic signal in groundwater. The average $\delta^{18}O$ in groundwater over the entire period was −9.84‰ and −9.86‰ for piezometers 8 and 12, respectively (SD = 0.1‰), while the average $\delta^{18}O$ for irrigation water was −10.2‰ (SE = 0.07‰ according to the same method for weighted mean isotope content as for rainfall). The weighted average of the input signal C_{in} was computed considering both rainfall and irrigation contributions:

$$C_{in} = \frac{\sum (C_r \times r) + \sum (C_{\text{Irr}} \times \text{Irr})}{\sum r + \sum \text{Irr}}$$

With r and Irr are rainfall and irrigations rates, respectively, and C_r and C_{irr} their respective isotope compositions.

This calculation yields a result of −9.66‰ (SE = 0.11‰), suggesting that the groundwater isotopic composition largely results from a mixing of rainfall and irrigation water, with the proportion of each driven by their respective volume. Based on this analysis, it is estimated that irrigation contributed approximately 85% of aquifer

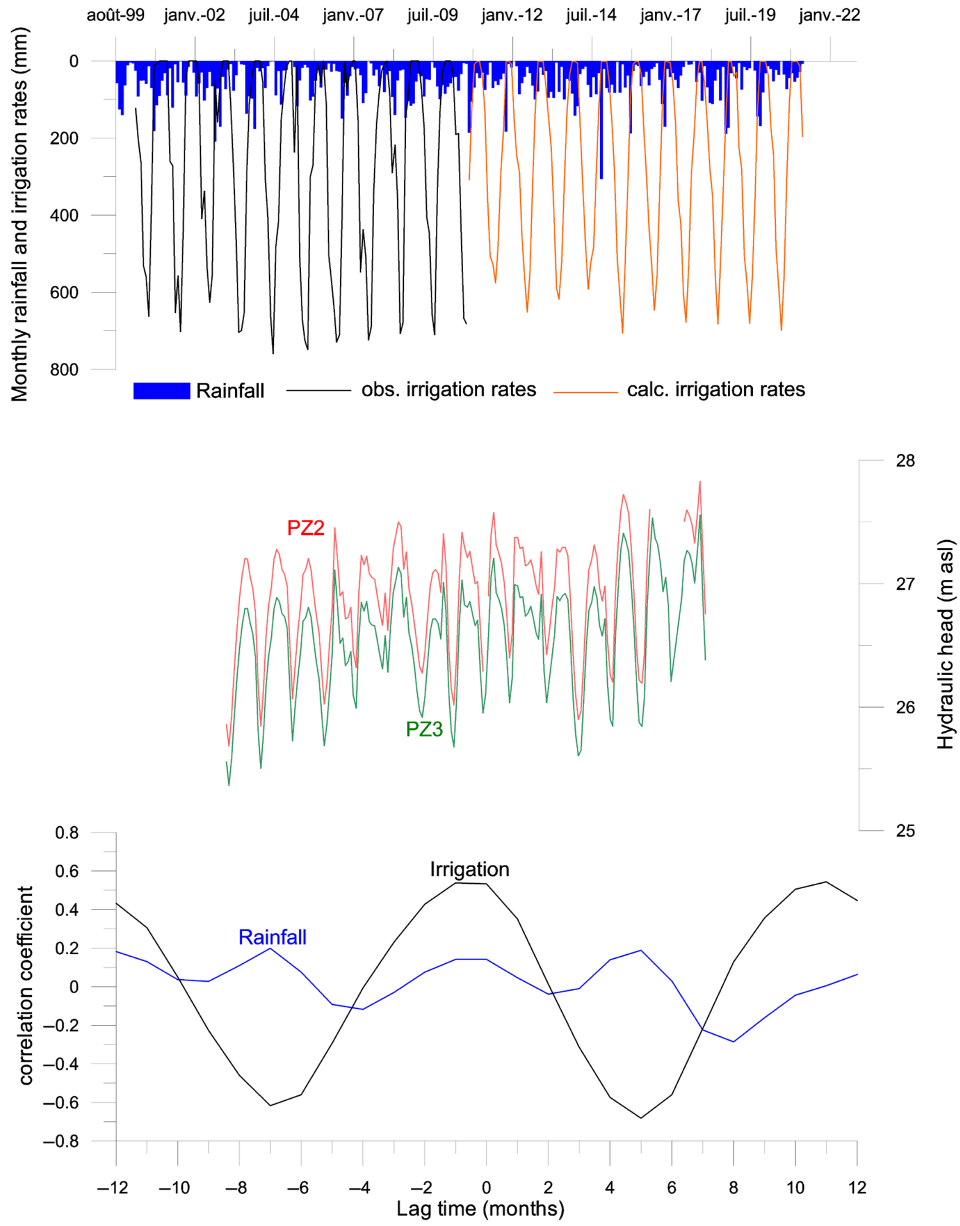

FIGURE 6 | (a) Time series of monthly inputs by irrigation and rainfall on the Avignon plain between August 1999 and March 2021. (b) Time series of monthly average water levels in the aquifer on the experimental plot (start of measurements January 2005). (c) Cross-correlation between rainfall/irrigation and groundwater level.

recharge. This figure is higher than that found in a previous study conducted upstream of our research area (Lacroix 1991). Notably, groundwater was slightly more depleted than the simple weighted average of the two input sources, indicating that the contribution of irrigation water to groundwater recharge might be slightly underestimated. To align the two values precisely, the irrigation rate would toned to be increased by about 20%.

3.4 | Modelling Isotopic Variations in Soil Water

3.4.1 | Simple Transfer (Single Function)

The simulation results using a single transfer function are summarised in Table 2.

The analysis was carried out using the monthly isotopic time series of rainwater as input, with 260 months of rainfall amounts and isotopic data available. Soil observations span up to 54 months (excluding gaps), starting from time step 58 (BPA4).

The calculated transit times showed a strong correlation with depth, ranging from 3 to 4 months at a depth of 19 cm to 35–37 months at 200 cm (Figure 9). The EMM and DM models were both consistent in this regard. Interestingly, the KGE optimisation metric was often more favourable for the EMM model, despite it having only one parameter (Table 2). However, the KGE value generally decreased with increasing soil depth. At 98 cm depth and below, the model struggled to capture the full variability observed (Figure 10).

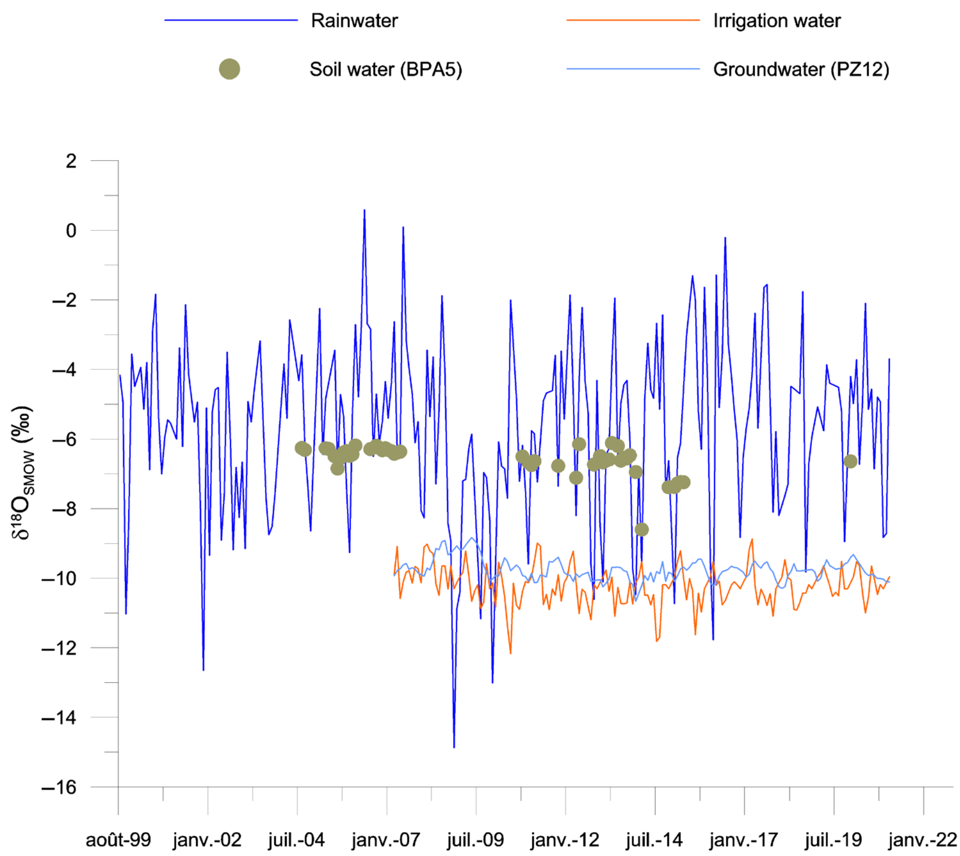

FIGURE 7 | Monthly isotopic time series ($\delta^{18}O_{SMOW}$) in rainwater, irrigation water, groundwater (ex. PZ12) and soil water (ex. BPA5).

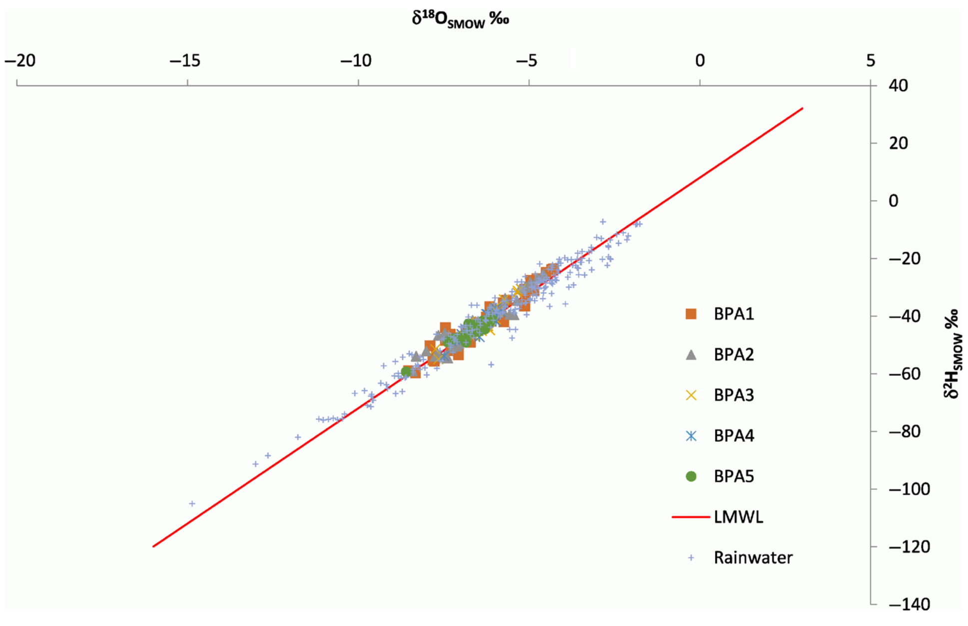

FIGURE 8 | Relation between $\delta^{18}O_{SMOW}$ and $\delta^{2}H_{SMOW}$ in soil waters and comparison with the local meteoric water line (LMWL).

3.4.2 | Binary Transfer (2 Parallel Transfer Functions)

To better capture the dynamics observed across all depths, we assumed that infiltration involved a combination of slow matrix flow and faster preferential flow. The matrix flow rate was modelled using a dispersive model (DM) to account for a proportion p of the total flow, while the preferential flow was represented by a piston flow model (PFM) with a transit time of 0 month (immediate response to monthly rainfall), covering the remaining proportion 1-p of the total flow.

TABLE 2 | Synthesis of the results of the EMM and DM transfer models for the 5 soil depths.

		BPA1	BPA2	BPA3	BPA4	BPA5
	Depth (m)	0.19	0.28	0.5	0.98	2
EMM	*T* (months)	3.2	4.3	10.3	15.1	34.8
	KGE	0.8	0.71	0.72	0.5	0.57
	RMSE	0.76	0.85	0.48	0.38	0.32
DM	*T* (months)	4.6	5	10.3	16.5	37.1
	DP	1.1	0.5	0.96	1	0.25
	KGE	0.78	0.71	0.59	0.05	0.44
	RMSE	0.74	0.73	0.57	0.57	0.33

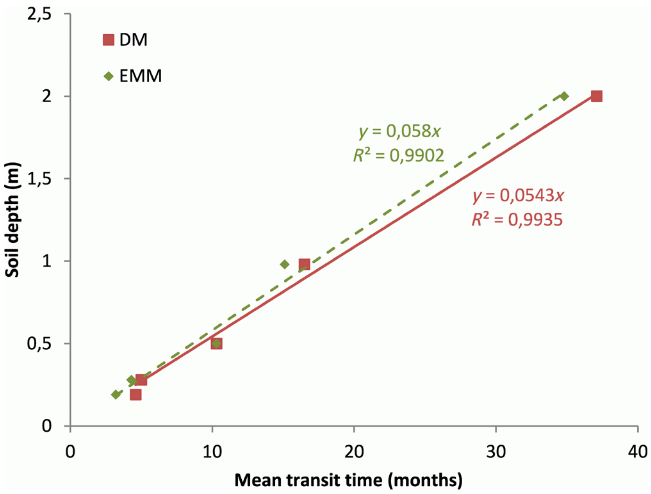

FIGURE 9 | Correlation between soil depth and mean transit time calculated with the EMM and DM models.

The simulations showed a marked improvement across all depths. The average transit times for the DM component of the model (matrix flow) ranged from 3.7 to 63.1 months (Table 3), resulting in an estimated percolation rate of 3 cm/month within the matrix (Figure 11). The preferential flow proportion remained consistently around 10%–15%, though this proportion gradually declined with depth. Incorporating preferential flow enhanced the model's ability to replicate the variations observed at the greatest depths (Figure 12). This result aligns with the soil characteristics outlined in Section 2. The mean transit time within the soil at a depth of 2 m was approximately 50 months, equating to an average infiltration rate of 4 cm/month. Consequently, the transit time for water at a depth of 4.5 m (mean depth of groundwater table), calculated from the infiltration rate, was approximately 120 months.

3.5 | Groundwater Isotopic Modelling

3.5.1 | Simple Transfer (Single Function)

The isotope models for groundwater were calibrated, accounting for the uncertainty in the irrigation rate. According to the results in Section 3, the irrigation rate was increased by 20% each month to maintain isotopic mass balance. However, the simulations yield generally poor outcomes. The KGE metric did not exceed 0.55, with the DM model providing the best performance (Table 4 and Figure 13). The EMM model's lower performance aligns with the context, given that the primary areas of irrigation recharge are located upstream of the observation point. The three models tested agreed on a mean transit time of approximately 9 months. It is noteworthy that this transit time is significantly shorter than the estimated transit time at the maximum depth observed in the soil.

3.5.2 | Binary Transfer (2 Parallel Transfer Functions)

The simulations were conducted as previously, with monthly irrigation rates increased by 20%. The initial binary model, which combined a DM function with a PFM function, did not yield convincing results. Notably, the most optimal simulation was achieved when all flow travelled through the dispersive part, effectively simplifying the model to a single DM simulation. The introduction of a fast piston-like flow did not enhance the model accuracy. Additional tests were performed pairing a DM function with an EMM, EPM or another DM function, but none of these combinations enhanced the simulation outcomes.

In a subsequent phase, two parallel simulations were conducted using two DM models (DM1 and DM2), based on the assumption that infiltration modalities might differ depending on whether the input source was irrigation (DM1) or rainfall (DM2). This technique yielded better results compared to those obtained with a single transfer function (Table 5). The groundwater exhibited a mean transit time of around 15 months: about 60 months for rainwater and approximately 8 months for irrigation, with irrigation comprising 85% of the recharge and rainwater 15%. It is worth noting that while the KGE reached an optimal value at $T2 = 56$ months, this metric displayed limited sensitivity to values beyond this (Figure 14).

The proposed model generally captured the isotopic variability within the aquifer (Figure 15), although it struggled to accurately represent the extreme values, particularly the low ones.

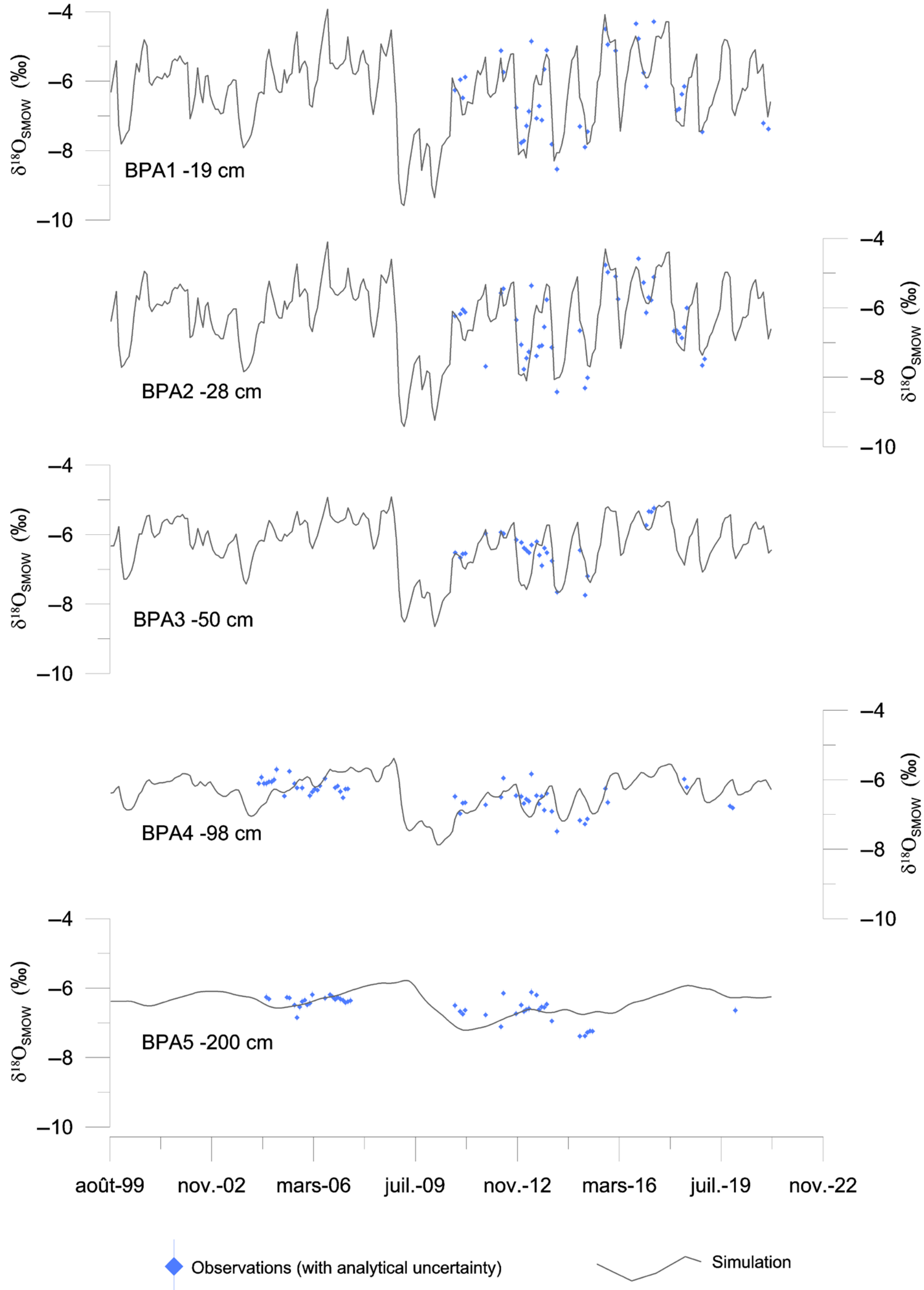

FIGURE 10 | Simulations of isotopic contents in soil water at different depths (example of the EMM model).

TABLE 3 | Summary of the results of the binary transfer model for the 5 soil depths (*p*, the proportion of the flow simulated by the DM part).

	BPA1	BPA2	BPA3	BPA4	BPA5
Depth (m)	0.19	0.28	0.5	0.98	2
$T(DM)$ (months)	3.7	4.5	13.6	30.5	63.1
DP	0.54	0.33	0.98	0.98	0.44
p	0.84	0.86	0.89	0.87	0.9
KGE	0.83	0.76	0.67	0.51	0.62
RMSE	0.67	0.66	0.5	0.38	0.29

4 | Discussion and Implications for Water Resource Management

4.1 | Influence of Soil Infiltrability Spatial Distribution and Hydrological Forcings on Recharge Processes

According to previous findings, a notable difference exists between the transit time derived from the soil data and that from groundwater data, even when considering only the "rainwater" component in the groundwater isotope transfer model.

One possible explanation for this discrepancy is the difference in spatial scales across the investigations. Soil data reflects local

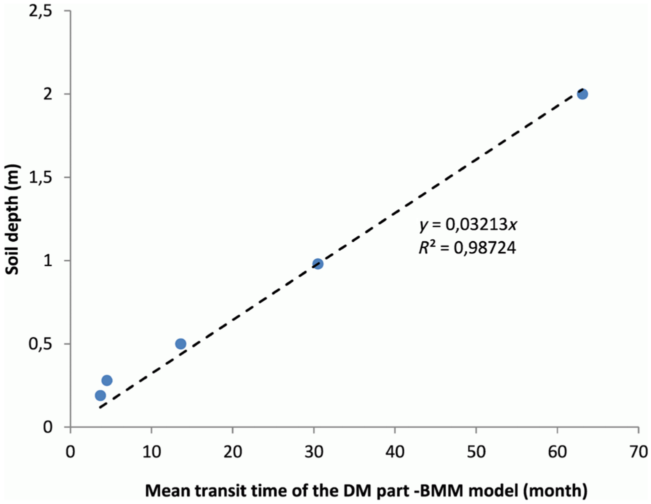

FIGURE 11 | Correlation between soil depth and mean transit time (DM part) calculated with the binary mixing model.

variations, whereas isotopic variations in groundwater result from the spatial integration of upstream mechanisms from the sampling point. Lithological sections at the experimental plot indicate surface layers of loams, silts and clays, 2–3 m thick, distributed unevenly across the plain. In the upstream areas, these low-permeability layers are relatively thin, thickening downstream, where the water table may be locally confined (Nofal et al. 2019). Measurements at the plot show relatively thick silts, which justify the need for longer infiltration duration. In contrast, groundwater measurements reveal infiltration in upstream areas with sparse or absent silts, explaining the shorter transit time calculated for groundwater.

The variation in transit time between the soil and water table is also influenced by how water is supplied to the soil. In gravity-fed irrigation, Ma et al. (2011) demonstrated that on the Crau plain, substantial quantities of irrigation water can reach the water table at 7 m depth within days. Forcing conditions vary considerably during rainfall events, particularly during intense Mediterranean autumn rainstorms (the so-called Cévenol events). Several authors have shown that the likelihood of preferential flows increases with rainfall amount or intensity (Jarvis et al. 2016; Wiekenkamp et al. 2016; Hu et al. 2019). Such rapid flows can occur under intense or heavy rainfall due to increased water pressure in the soil, especially within macropores (Li et al. 2020). Consensus on the specific thresholds for initiating these processes remains elusive due to the range of influencing factors (Weiler 2017). The relationship between the nature of the input function and recharge efficiency, as identified by Olioso et al. (2013), supports separating rainfall and irrigation in recharge model. This finding confirms the choice made here to distinguish these two flows in the isotope transfer model.

4.2 | Challenges for Modelling and Broader Methodological Implications

Our findings, which indicate discrepancies in model accuracy when dealing with complex recharge sources, suggest that models need to be refined to better capture preferential flows and the effects of irrigation practices. Figure 15 shows that the model struggled to fully capture the isotopic variability observed in groundwater, particularly poorly simulating depleted values. These depleted values were frequently recorded in irrigation water (Figure 8). However, such poorly simulated points consistently occurred at the start of the calendar year – in January, February, or March – when irrigation activities are theoretically absent. Additionally, monthly isotope monitoring of rainwater occasionally revealed even more negative values than those found in irrigation water.

The model's difficulties in reproducing observations may be explained by its inadequate structural alignment with field processes. As previously stated, the proposed binary model assumes different behaviours between recharge from rainfall and recharge from irrigation. For irrigation, the relatively constant water supply conditions justify the use of a single transfer function. Rainfall infiltration processes differ depending on the rainfall amount and intensity. A binary sub-model for rainfall, with two transfer functions activated according to a rainfall threshold, could be considered. This model structure results increases the number of parameters from 4 to 7 when 2 dispersive functions are used for the soil. Although this model was tested, it did not improve the simulations, especially for the extreme values.

Another issue to consider is the time scale used in the analysis. For practical reasons, including sampling and analytical constraints, the study was conducted using a monthly time scale. Yet, the relevant processes could be occurring on time scales that differ significantly from the one used here. During an experiment on the measurement site, labelled water was used to simulate rainfall, demonstrating that a small amount of rainwater could reach the water table in just a few hours (Garel et al. 2007). Furthermore, with regard to groundwater–river exchange, the parameters governing water transport (such as water velocity and dispersivity) were found to depend on the chosen time scale, likely due to the different mechanisms involved (Poulain et al. 2021). In this study, the groundwater samples were collected periodically, which may not be reflective of the monthly averages. The simulated inaccuracies could arise due to rapid infiltration following preceding heavy rainfall events, depending on the time of sampling. To better detect these phenomena, short-term monitoring (daily) should be conducted during the intense rainfall events that are typically observed in autumn.

The study highlights the challenges in using lumped parameter models (LPM) to simulate groundwater recharge processes under the dual influences of rainfall and irrigation. This insight is applicable to a wide audience of hydrologists and water resource managers who rely on models to predict water availability. In particular, this study's approach of using long-term isotopic data to calibrate models provides a valuable example of how integrating detailed field data can improve model accuracy. Future research efforts could build on this work by incorporating high-frequency monitoring data and more complex modelling approaches to better capture the full variability of groundwater recharge processes.

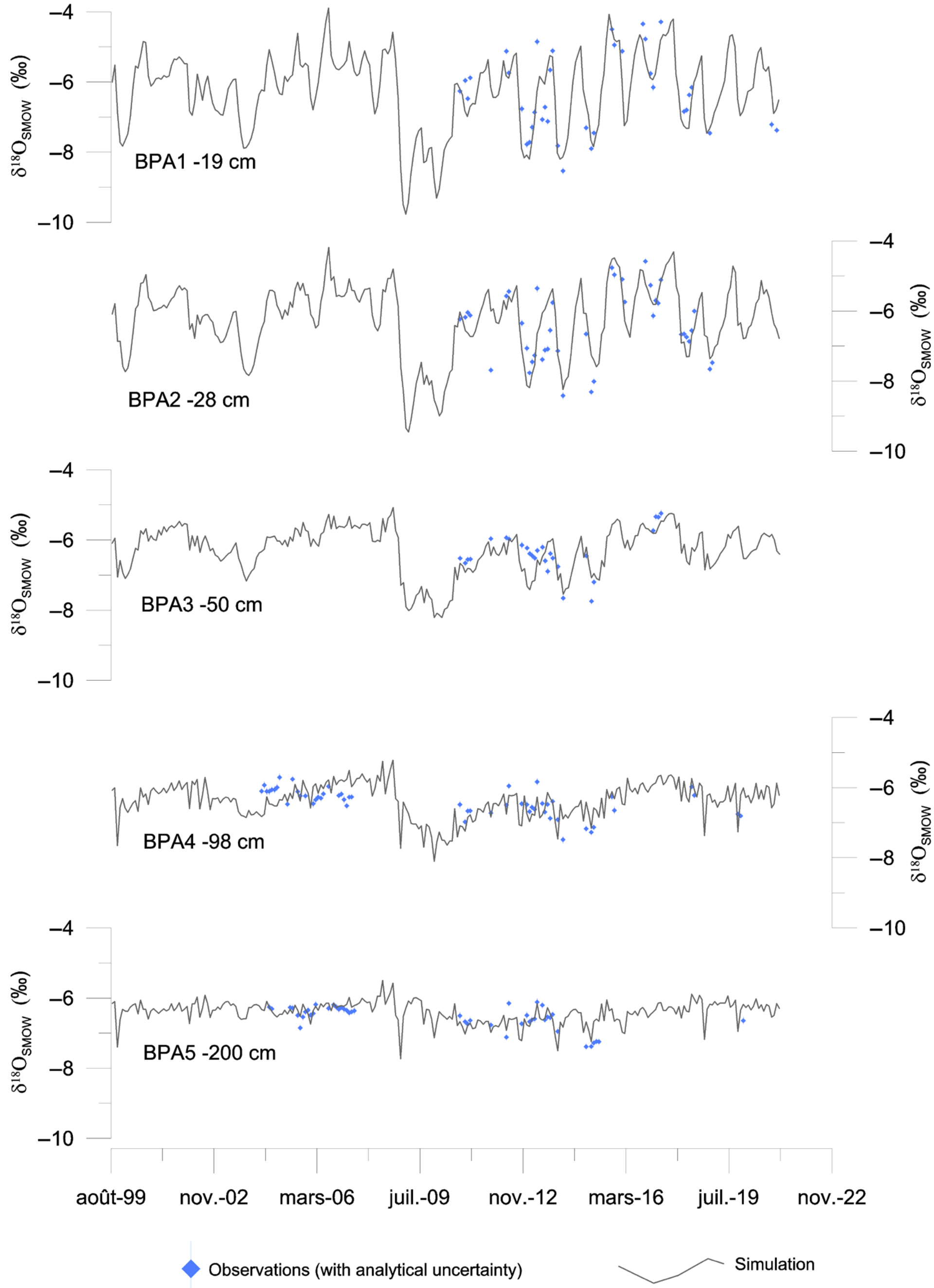

FIGURE 12 | Simulations of isotope contents in soil water at different depths (DM-PFM binary mixing model).

4.3 | Implications for Global Water Resource Management and Irrigation Practices in the Context of Climate Change

Gravity-fed irrigation systems, while traditionally perceived as inefficient due to water loss through evaporation and surface runoff, are shown to play a crucial role in aquifer recharge. For instance, Bouimouass et al. (2022) and Masseroni et al. (2017) highlight how traditional irrigation methods sustain groundwater quality and recharge despite their high water consumption. But the broader hydrological implications of the present study extend beyond the Mediterranean region. It contributes to a body of knowledge that emphasises the need to rethink water management practices in arid and semi-arid regions globally. As water availability becomes increasingly uncertain, this research offers insights that could help develop new strategies for aquifer management, potentially applicable in regions like the U.S. southwest, sub-saharan Africa, middle east and parts of Asia (Gordon et al. 2020; Darko et al. 2020; Bouimouass et al. 2020; Karimov et al. 2021).

The observation that gravity-fed irrigation contributes 85% of the aquifer recharge in the Avignon plain challenges the conventional wisdom that modern, high-efficiency irrigation systems like drip or sprinkler irrigation are always preferable. While these systems save water at the surface, they may reduce the

TABLE 4 | Results of the fitting for the groundwater with the EMM, EPM and DM models.

EMM	T (months)	9
	KGE	0.28
	RMSE	0.31
EPM	T (months)	9
	n	1.4
	KGE	0.47
	RMSE	0.29
DM	T (months)	8.4
	DP	0.11
	KGE	0.55
	RMSE	0.28

natural groundwater recharge that occurs through more traditional flood irrigation methods. This insight could inform water management strategies globally, suggesting a need for a more nuanced approach that balances surface water efficiency with the benefits of aquifer recharge. These results provide evidence that MAR techniques could be effectively integrated into traditional irrigation systems. For example, using irrigation canals during non-irrigation periods to artificially recharge aquifers could mitigate the effects of extended droughts. The relevance of this finding is particularly important as many regions are now exploring strategies to adapt to the twin challenges of increasing agricultural demand and shrinking water resources due to climate change (Alaanuloluwa Ikhuoso et al. 2020; Sivakumar 2021; Martínez-Valderrama et al. 2023).

From a policy perspective, the results underscore the need for integrated water management strategies that account for both

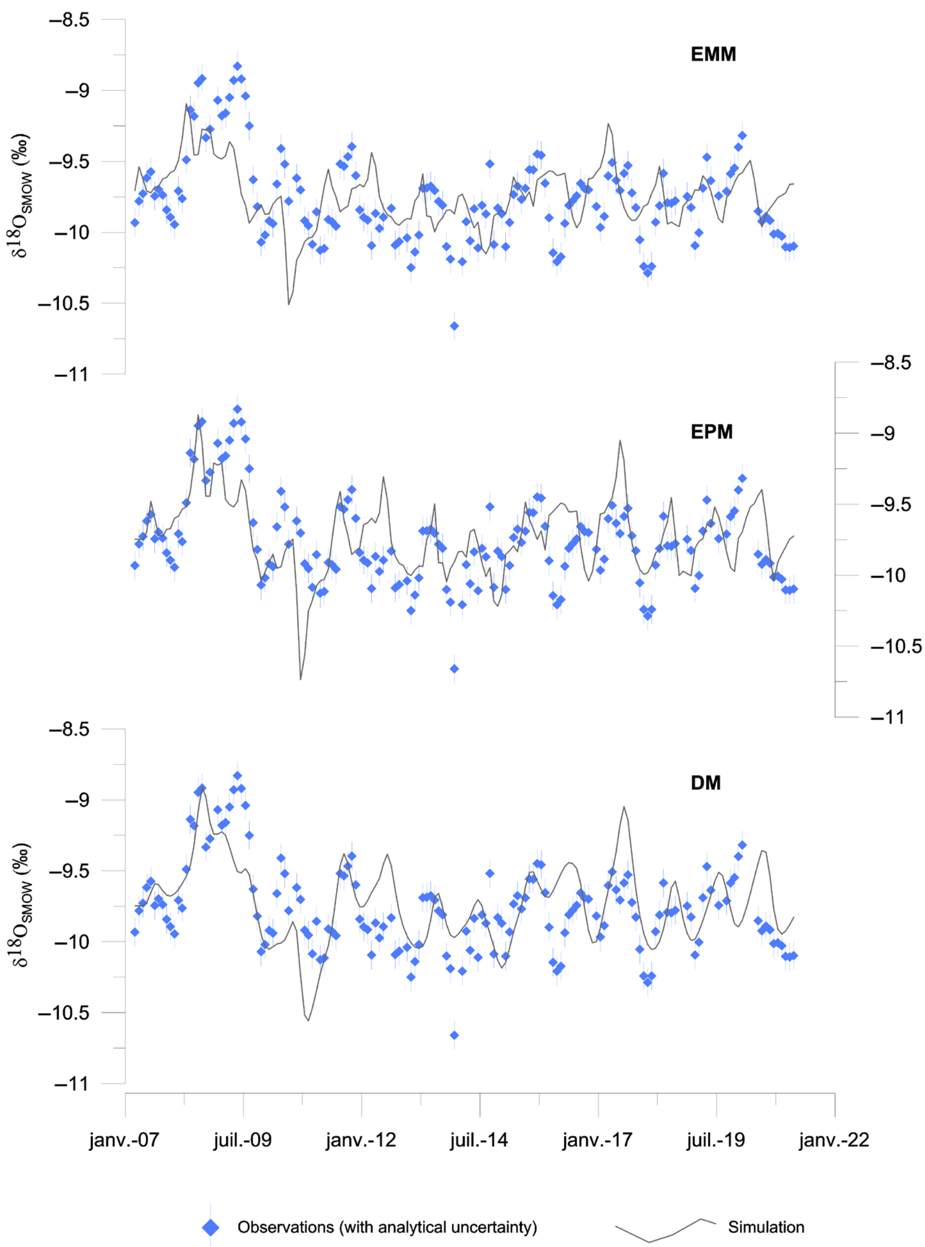

FIGURE 13 | Isotopic simulations of groundwater with the EMM, EPM and DM models.

TABLE 5 | Summary of results for the binary model (IRR + RAIN) for the groundwater case.

$T1$ (IRR) (months)	7.9
$T2$ (RAIN) (months)	56
D1 (IRR)	0.11
D2 (RAIN)	0.11
KGE	0.64
RMSE	0.26

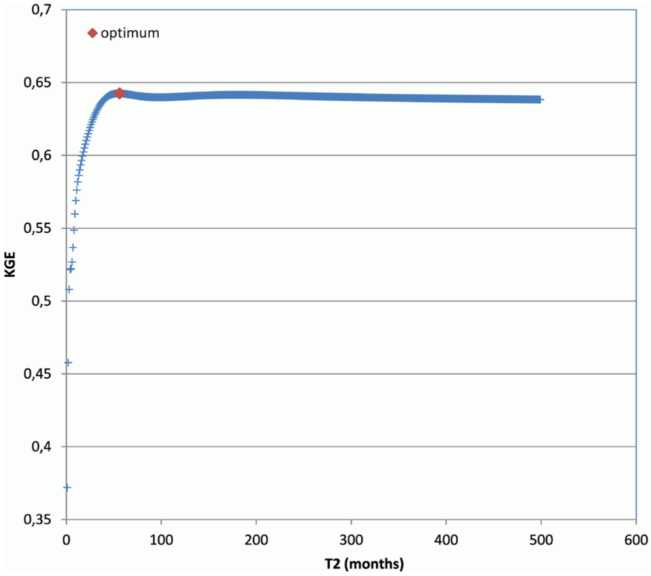

FIGURE 14 | Variation of KGE as a function of T2.

surface and groundwater resources. Many regions currently manage these resources separately, often focusing on surface water efficiency at the expense of groundwater recharge. This study suggests that a more holistic approach is needed – one that considers the indirect benefits of traditional irrigation practices in recharging aquifers. Policymakers can use these findings to develop water-saving irrigation strategies that do not compromise groundwater recharge. For example, adapting irrigation schedules to maximise recharge during periods of lower agricultural demand or exploring dual-purpose infrastructure (irrigation and recharge) could help mitigate water scarcity. This approach aligns with global efforts to implement sustainable development goals (SDGs), particularly SDG 6, which focuses on ensuring the availability and sustainable management of water and sanitation for all (United Nations 2018).

The findings of this study indicate that the preservation of these systems, or the implementation of modernisation measures, can serve as an indirect yet effective instrument for the enhancement of global groundwater management.

5 | Conclusion

This study provides new insights into the hydrological processes of groundwater recharge under the combined influence of gravity-fed irrigation and natural rainfall in a Mediterranean alluvial aquifer. Using long-term isotopic monitoring and lumped parameter models, we quantified the significant contribution of irrigation – approximately 85% – to annual aquifer recharge. This finding underscores the crucial role that traditional irrigation systems play in enhancing groundwater resources, even in semi-arid regions where water is scarce. The modelling results revealed distinct infiltration dynamics between irrigation and

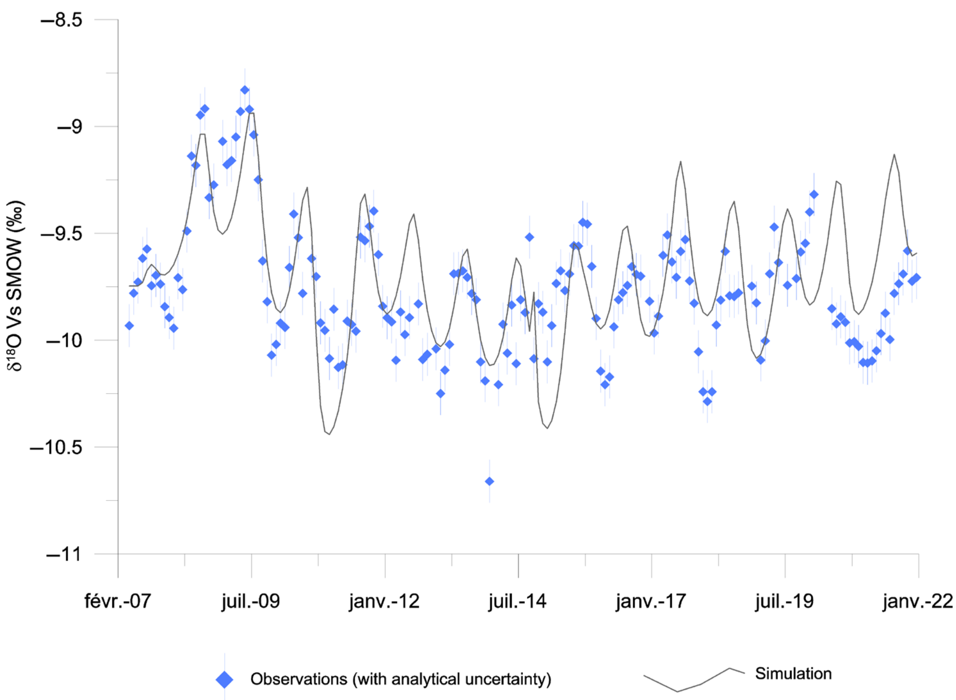

FIGURE 15 | Isotopic simulations of groundwater with the BMM model (IRR + RAIN).

rainfall sources, with faster transit times associated with irrigation flows, highlighting the impact of irrigation practices on recharge efficiency.

Our approach demonstrates the utility of isotopic techniques for distinguishing recharge sources, offering a cost-effective and scalable method for understanding recharge processes in regions with limited hydrological data. These findings have broad implications for water management policies, particularly in water-stressed regions facing climate change. To sustain groundwater levels, we recommend that policymakers consider both the water-saving benefits of modern irrigation and the recharge benefits of traditional methods. Future research should focus on high-frequency monitoring and refined models to better capture recharge variability and support adaptive water management strategies in diverse agricultural contexts worldwide.

Acknowledgements

The authors express their gratitude to Guillaume Cinkus for his assistance in enhancing the quality of the figures and for the valuable discussions on the optimisation metrics. The four reviewers are thanked for the time they spent on the manuscript and for their thoughtful and valuable comments.

Data Availability Statement

The data that support the findings of this study are available from the corresponding author upon reasonable request.

References

AIRMF. 2009. "L'Agriculture Irriguée Méditerranéenne, Une Source de Richesse au Cœur Des Enjeux du Développement Durable|AIRMF." https://www.airmf.fr/publication-2/.

Alaanuloluwa Ikhuoso, O., M. J. Adegbeye, M. M. Y. Elghandour, M. Mellado, S. N. Al-Dobaib, and A. Z. M. Salem. 2020. "Climate Change and Agriculture: the Competition for Limited Resources Amidst Crop Farmers-Livestock Herding Conflict in Nigeria—A Review." *Journal of Cleaner Production* 272: 123104. https://doi.org/10.1016/j.jclepro.2020.123104.

Ali, A. A., D. Q. Tran, K. F. Kovacs, and H. E. Dahlke. 2023. "Hydro-Economic Modeling of Managed Aquifer Recharge in the Lower Mississippi." *JAWRA Journal of the American Water Resources Association* 59: 1413–1434. https://doi.org/10.1111/1752-1688.13141.

Aspe, C. 2012. *De L'eau Agricole à L'eau Environnementale, in: De L'eau Agricole à L'eau Environnementale*, 7–17. Versailles: Natures Sociales. Éditions Quæ. https://doi.org/10.3917/quae.aspe.2012.01.0007.

Bartyzel, J., and K. Rozanski. 2016. "Dating of Young Groundwater Using Four Anthropogenic Trace Gases (SF6, SF5CF3, CFC-12 and Halon-1301): Methodology and First Results†." *Isotopes in Environmental and Health Studies* 52: 393–404. https://doi.org/10.1080/10256016.2015.1135137.

Batlle-Aguilar, J., E. W. Banks, O. Batelaan, R. Kipfer, M. S. Brennwald, and P. G. Cook. 2017. "Groundwater Residence Time and Aquifer Recharge in Multilayered, Semi-Confined and Faulted Aquifer Systems Using Environmental Tracers." *Journal of Hydrology* 546: 150–165. https://doi.org/10.1016/j.jhydrol.2016.12.036.

Blavoux, B., P. Lachassagne, A. Henriot, et al. 2013. "A Fifty-Year Chronicle of Tritium Data for Characterising the Functioning of the Evian and Thonon (France) Glacial Aquifers." *Journal of Hydrology* 494: 116–133. https://doi.org/10.1016/j.jhydrol.2013.04.029.

Bogner, C., M. Mirzaei, S. Ruy, and B. Huwe. 2013. "Microtopography, Water Storage and Flow Patterns in a Fine-Textured Soil Under Agricultural Use." *Hydrological Processes* 27: 1797–1806. https://doi.org/10.1002/hyp.9337.

Bouimouass, H., Y. Fakir, S. Tweed, and M. Leblanc. 2020. "Groundwater Recharge Sources in Semiarid Irrigated Mountain Fronts." *Hydrological Processes* 34: 1598–1615. https://doi.org/10.1002/hyp.13685.

Bouimouass, H., Y. Fakir, S. Tweed, H. Sahraoui, M. Leblanc, and A. Chehbouni. 2022. "Traditional Irrigation Practices Sustain Groundwater Quality in a Semiarid Piedmont." *Catena* 210: 105923.

Bouwer, H. 2000. "Integrated Water Management: Emerging Issues and Challenges." *Agricultural Water Management* 45: 217–228. https://doi.org/10.1016/S0378-3774(00)00092-5.

Bredehoeft, J. D., S. S. Papadopulos, and H. H. Cooper Jr. 1982. "Groundwater: The Water Budget Myth." *Scientific Basis of Water Resource Management* 51: 57.

Brillard, J., C. M. Dupont, O. Berge, et al. 2015. "The Water Cycle, a Potential Source of the Bacterial Pathogen *Bacillus cereus*." *BioMed Research International* 2015: 356928. https://doi.org/10.1155/2015/356928.

Cartwright, I., D. Cendón, M. Currell, and K. Meredith. 2017. "A Review of Radioactive Isotopes and Other Residence Time Tracers in Understanding Groundwater Recharge: Possibilities, Challenges, and Limitations." *Journal of Hydrology* 555: 797–811. https://doi.org/10.1016/j.jhydrol.2017.10.053.

Chen, C., X. Zou, A. K. Singh, et al. 2021. "Effects of Hillslope Position on Soil Water Infiltration and Preferential Flow in Tropical Forest in Southwest China." *Journal of Environmental Management* 299: 113672. https://doi.org/10.1016/j.jenvman.2021.113672.

Chmielarski, M., S. Dogramaci, P. G. Cook, et al. 2024. "Identifying the Influence of Episodic Events on Groundwater Recharge in Semi-Arid Environments Using Environmental Tracers." *Journal of Hydrology* 633: 130848. https://doi.org/10.1016/j.jhydrol.2024.130848.

Cinkus, G., N. Mazzilli, H. Jourde, et al. 2023. "When Best Is the Enemy of Good – Critical Evaluation of Performance Criteria in Hydrological Models." *Hydrology and Earth System Sciences* 27: 2397–2411. https://doi.org/10.5194/hess-27-2397-2023.

Clark, M. P., R. M. Vogel, J. R. Lamontagne, et al. 2021. "The Abuse of Popular Performance Metrics in Hydrologic Modeling." *Water Resources Research* 57: e2020WR029001. https://doi.org/10.1029/2020WR029001.

Cook, P. G., G. R. Walker, G. Buselli, I. Potts, and A. R. Dodds. 1992. "The Application of Electromagnetic Techniques to Groundwater Recharge Investigations." *Journal of Hydrology* 130: 201–229. https://doi.org/10.1016/0022-1694(92)90111-8.

Cuthbert, M. O., R. I. Acworth, M. S. Andersen, et al. 2016. "Understanding and Quantifying Focused, Indirect Groundwater Recharge From Ephemeral Streams Using Water Table Fluctuations." *Water Resources Research* 52: 827–840. https://doi.org/10.1002/2015WR017503.

Darko, R. O., J. Liu, S. Yuan, L. K. Sam-Amoah, and H. Yan. 2020. "Irrigated Agriculture for Food Self-Sufficiency in the Sub-Saharan African Region." *International Journal of Agricultural and Biological Engineering* 13: 1–12. https://doi.org/10.25165/ijabe.v13i3.4397.

Dillon, P., S. Toze, D. Page, et al. 2010. "Managed Aquifer Recharge: Rediscovering Nature as a Leading Edge Technology." *Water Science and Technology* 62: 2338–2345. https://doi.org/10.2166/wst.2010.444.

Eberts, S. M., J. K. Böhlke, L. J. Kauffman, and B. C. Jurgens. 2012. "Comparison of Particle-Tracking and Lumped-Parameter Age-Distribution Models for Evaluating Vulnerability of Production Wells to Contamination." *Hydrogeology Journal* 20: 263–282. https://doi.org/10.1007/s10040-011-0810-6.

Edwards, E. C., T. Harter, G. E. Fogg, B. Washburn, and H. Hamad. 2016. "Assessing the Effectiveness of Drywells as Tools for Stormwater

Management and Aquifer Recharge and Their Groundwater Contamination Potential." *Journal of Hydrology* 539: 539–553. https://doi.org/10.1016/j.jhydrol.2016.05.059.

Felfelani, F., J. Hughes, F. Chen, et al. 2024. "Simulation of Groundwater-Flow Dynamics in the U.S. Northern High Plains Driven by Multi-Model Estimates of Surficial Aquifer Recharge." *Journal of Hydrology* 630: 130703. https://doi.org/10.1016/j.jhydrol.2024.130703.

Fórizs, I., T. Berecz, Z. Molnár, and M. Süveges. 2005. "Origin of Shallow Groundwater of Csepel Island (South of Budapest, Hungary, River Danube): Isotopic and Chemical Approach." *Hydrological Processes* 19: 3299–3312. https://doi.org/10.1002/hyp.5971.

Ganot, Y., R. Holtzman, N. Weisbrod, I. Nitzan, Y. Katz, and D. Kurtzman. 2017. "Monitoring and Modeling Infiltration–Recharge Dynamics of Managed Aquifer Recharge With Desalinated Seawater." *Hydrology and Earth System Sciences* 21: 4479–4493. https://doi.org/10.5194/hess-21-4479-2017.

Garel, E., V. Marc, S. Ruy, et al. 2007. "Infi Ltration Processes and Impact on Shallow Groundwater in Agricultural Dry Land Areas." In *Presented at the Advances in Isotope Hydrology and Its Role in Sustainable Water Resources Management*, 567–575. Vienna: IAEA.

Gee, G. W., Z. F. Zhang, S. W. Tyler, W. H. Albright, and M. J. Singleton. 2005. "Chloride Mass Balance: Cautions in Predicting Increased Recharge Rates." *Vadose Zone Journal* 4: 72–78. https://doi.org/10.2136/vzj2005.0072a.

Gerber, C., R. Vaikmäe, W. Aeschbach, et al. 2017. "Using 81Kr and Noble Gases to Characterize and Date Groundwater and Brines in the Baltic Artesian Basin on the One-Million-Year Timescale." *Geochimica et Cosmochimica Acta* 205: 187–210. https://doi.org/10.1016/j.gca.2017.01.033.

Godwin, I. A., M. L. Reba, D. L. Leslie, R. F. Adams, and J. R. Rigby. 2022. "Feasibility of Farm-Scale Infiltration Galleries for Managed Aquifer Recharge in an Agricultural Alluvial Aquifer of Northeast Arkansas." *Agricultural Water Management* 264: 107531. https://doi.org/10.1016/j.agwat.2022.107531.

Gogolev, M. I. 2002. "Assessing Groundwater Recharge With Two Unsaturated Zone Modeling Technologies." *Environmental Geology* 42: 248–258. https://doi.org/10.1007/s00254-001-0494-7.

Gong, C., P. G. Cook, R. Therrien, W. Wang, and P. Brunner. 2023. "On Groundwater Recharge in Variably Saturated Subsurface Flow Models." *Water Resources Research* 59: e2023WR034920. https://doi.org/10.1029/2023WR034920.

Gordon, B. L., G. B. Paige, S. N. Miller, N. Claes, and A. D. Parsekian. 2020. "Field Scale Quantification Indicates Potential for Variability in Return Flows From Flood Irrigation in the High Altitude Western US." *Agricultural Water Management* 232: 106062. https://doi.org/10.1016/j.agwat.2020.106062.

Gourdol, L., M. K. Stewart, U. Morgenstern, and L. Pfister. 2024. "Short High-Accuracy Tritium Data Time Series for Assessing Groundwater Mean Transit Times in the Vadose and Saturated Zones of the Luxembourg Sandstone Aquifer." *Hydrology and Earth System Sciences* 28: 3519–3547. https://doi.org/10.5194/hess-28-3519-2024.

Gupta, H. V., H. Kling, K. K. Yilmaz, and G. F. Martinez. 2009. "Decomposition of the Mean Squared Error and NSE Performance Criteria: Implications for Improving Hydrological Modelling." *Journal of Hydrology* 377: 80–91. https://doi.org/10.1016/j.jhydrol.2009.08.003.

Healy, R. W. 2010. *Estimating Groundwater Recharge*. Cambridge: Cambridge University Press. https://doi.org/10.1017/CBO9780511780745.

Hu, H., J. Wen, Z. Peng, et al. 2019. "High-Frequency Monitoring of the Occurrence of Preferential Flow on Hillslopes and Its Relationship With Rainfall Features, Soil Moisture and Landscape." *Hydrological Sciences Journal* 64: 1385–1396. https://doi.org/10.1080/02626667.2019.1638513.

Ifediegwu, I. S. 2020. "Groundwater Recharge Estimation Using Chloride Mass Balance: A Case Study of Nsukka Local Government Area of Enugu State, Southeastern, Nigeria." *Modeling Earth Systems and Environment* 6: 799–810. https://doi.org/10.1007/s40808-019-00707-7.

Jackson, E. K., W. Roberts, B. Nelsen, G. P. Williams, E. J. Nelson, and D. P. Ames. 2019. "Introductory Overview: Error Metrics for Hydrologic Modelling – A Review of Common Practices and an Open Source Library to Facilitate Use and Adoption." *Environmental Modelling and Software* 119: 32–48. https://doi.org/10.1016/j.envsoft.2019.05.001.

Jarvis, N., J. Koestel, and M. Larsbo. 2016. "Understanding Preferential Flow in the Vadose Zone: Recent Advances and Future Prospects." *Vadose Zone Journal* 15: 1–11. https://doi.org/10.2136/vzj2016.09.0075.

Jie, F., L. Fei, S. Li, et al. 2022. "Quantitative Effects of Vadose Zone Thickness on Delayed Recharge of Groundwater for an Irrigation District in an Arid Area of Northwest China." *Journal of Hydrology: Regional Studies* 40: 101022. https://doi.org/10.1016/j.ejrh.2022.101022.

Jurgens, B. C., J. K. Böhlke, and S. M. Eberts. 2012. "TracerLPM (Version 1): An Excel® Workbook for Interpreting Groundwater Age Distributions From Environmental Tracer Data, United States Geological Survey Techniques and Methods Report 4-F3, 60." Rest. Va. USA 72p.

Karimov, A. K., R. H. Toshev, R. Karshiev, and A. A. Karimov. 2021. "Water–Energy Nexus in Central Asia's Lift Irrigation Schemes: Multi-Level Linkages." *Renewable and Sustainable Energy Reviews* 147: 111148. https://doi.org/10.1016/j.rser.2021.111148.

Kármán, K., P. Maloszewski, J. Deák, I. Fórizs, and C. Szabó. 2014. "Transit Time Determination for a Riverbank Filtration System Using Oxygen Isotope Data and the Lumped-Parameter Model." *Hydrological Sciences Journal* 59: 1109–1116. https://doi.org/10.1080/02626667.2013.808345.

Kirchner, J. W., and S. T. Allen. 2020. "Seasonal Partitioning of Precipitation Between Streamflow and Evapotranspiration, Inferred From End-Member Splitting Analysis." *Hydrology and Earth System Sciences* 24: 17–39. https://doi.org/10.5194/hess-24-17-2020.

Koeniger, P., M. Gaj, M. Beyer, and T. Himmelsbach. 2016. "Review on Soil Water Isotope-Based Groundwater Recharge Estimations." *Hydrological Processes* 30: 2817–2834. https://doi.org/10.1002/hyp.10775.

Kuhfuss, L., and S. Loubier. 2013. "Comment Évaluer Les Services Rendus Par Les Réseaux D'irrigation? APPLICATION au Cas de la Recharge De Nappe." *Sciences Eaux and Territoires Pour Tous* 2: 70–77.

Kühnhammer, K., A. Dahlmann, A. Iraheta, et al. 2022. "Continuous In Situ Measurements of Water Stable Isotopes in Soils, Tree Trunk and Root Xylem: Field Approval." *Rapid Communications in Mass Spectrometry* 36: e9232. https://doi.org/10.1002/rcm.9232.

Lacroix, M. 1991. "Impact de L'irrigation Sur un Aquifere Alluvial. Dynamique du Système Basse Durance: Nitrates et Isotopes (Cartographie); Piezometrie (Modélisation Mathematique) Besançon."

Lacroix, M., H. Q. Wang, and B. Blavoux. 1996. "Water-Table Modelling to Estimate Irrigation Losses: Application to the Lower Durance, France." *Agricultural Water Management* 30: 283–300. https://doi.org/10.1016/0378-3774(95)01227-3.

Le Duy, N., N. V. Dung, I. Heidbüchel, et al. 2019. "Identification of Groundwater Mean Transit Times of Precipitation and Riverbank Infiltration by Two-Component Lumped Parameter Models." *Hydrological Processes* 33: 3098–3118. https://doi.org/10.1002/hyp.13549.

Li, J., Y.-K. Zhang, Z. Zhou, Y. Guo, J. Zhao, and X. Liang. 2024. "Using Multiple Isotopes to Determine Groundwater Source, Age, and Renewal Rate in the Beishan Preselected Area for Geological Disposal of High-Level Radioactive Waste in China." *Journal of Hydrology* 629: 130592. https://doi.org/10.1016/j.jhydrol.2023.130592.

Li, M., J. Yao, and J. Cheng. 2020. "Study on the Preferential Flow Characteristics Under Different Precipitation Amounts in Simian Mountain Grassland of China." *Watermark* 12: 3489. https://doi.org/10.3390/w12123489.

Livet, R. 1980. "Irrigation et Sociétés Dans le Monde Méditerranéen." *Méditerranée* 39: 3–11. https://doi.org/10.3406/medit.1980.1935.

Lorenzo, M. N., and I. Alvarez. 2022. "Future Changes of Hot Extremes in Spain: Towards Warmer Conditions." *Natural Hazards* 113: 383–402. https://doi.org/10.1007/s11069-022-05306-x.

Ma, D., C. Doussan, A. Chapelet, F. Charron, and A. Olioso. 2011. "Monitoring Soil to Groundwater Preferential Flow During Border Irrigation Using Time-Lapse ERT." *Geophysical Research Abstracts* 13: EGU2011–9097.

Maliva, R. G., E. A. Clayton, and T. M. Missimer. 2009. "Application of Advanced Borehole Geophysical Logging to Managed Aquifer Recharge Investigations." *Hydrogeology Journal* 17: 1547–1556. https://doi.org/10.1007/s10040-009-0437-z.

Maloszewski, P., S. Maciejewski, C. Stumpp, W. Stichler, P. Trimborn, and D. Klotz. 2006. "Modelling of Water Flow Through Typical Bavarian Soils: 2 Environmental Deuterium Transport." *Hydrological Sciences Journal* 51: 298–313. https://doi.org/10.1623/hysj.51.2.298.

Maloszewski, P., W. Rauert, P. Trimborn, A. Herrmann, and R. Rau. 1992. "Isotope Hydrological Study of Mean Transit Times in an Alpine Basin (Wimbachtal, Germany)." *Journal of Hydrology* 140: 343–360.

Małoszewski, P., and A. Zuber. 1982. "Determining the Turnover Time of Groundwater Systems With the Aid of Environmental Tracers: 1 Models and Their Applicability." *Journal of Hydrology* 57: 207–231. https://doi.org/10.1016/0022-1694(82)90147-0.

Maloszewski, P., and A. Zuber. 1996. "Lumped Parameter Models for Interpretation of Environmental Tracer Data." In *Manual on the Mathematical Models in Isotope Hydrogeology*, 9–59. Vienna: IAEA.

Martínez-Valderrama, J., J. Olcina, G. Delacámara, E. Guirado, and F. T. Maestre. 2023. "Complex Policy Mixes Are Needed to Cope With Agricultural Water Demands Under Climate Change." *Water Resources Management* 37: 2805–2834. https://doi.org/10.1007/s11269-023-03481-5.

Masseroni, D., S. Ricart, F. R. De Cartagena, et al. 2017. "Prospects for Improving Gravity-Fed Surface Irrigation Systems in Mediterranean European Contexts." *Watermark* 9: 20.

Mayer, A., J. Sültenfuß, Y. Travi, et al. 2014. "A Multi-Tracer Study of Groundwater Origin and Transit-Time in the Aquifers of the Venice Region." *Applied Geochemistry* 50: 177–198. https://doi.org/10.1016/j.apgeochem.2013.10.009.

Müller, T., K. Osenbrück, G. Strauch, et al. 2016. "Use of Multiple Age Tracers to Estimate Groundwater Residence Times and Long-Term Recharge Rates in Arid Southern Oman." *Applied Geochemistry* 74: 67–83. https://doi.org/10.1016/j.apgeochem.2016.08.012.

Musgrove, M., B. C. Jurgens, and S. P. Opsahl. 2023. "Karst Groundwater Vulnerability Determined by Modeled Age and Residence Time Tracers." *Geophysical Research Letters* 50: e2023GL102853. https://doi.org/10.1029/2023GL102853.

Niswonger, R. G., E. D. Morway, E. Triana, and J. L. Huntington. 2017. "Managed Aquifer Recharge Through Off-Season Irrigation in Agricultural Regions." *Water Resources Research* 53: 6970–6992. https://doi.org/10.1002/2017WR020458.

Nobles, M. M., L. P. Wilding, and H. S. Lin. 2010. "Flow Pathways of Bromide and Brilliant Blue FCF Tracers in Caliche Soils." *Journal of Hydrology* 393: 114–122. https://doi.org/10.1016/j.jhydrol.2010.03.014.

Nofal, S. 2014. "Etude du Fonctionnement Hydrodynamique de la Nappe Alluviale D'Avignon. Impact de L'Usage du Sol Sur Les Mécanismes de Recharge. Avignon Université."

Nofal, S., B. Blavoux, A. L. Cognard-Plancq, V. Marc, and Y. Travi. 2010. "L'approvisionnement en Eau Potable de la Ville d'Avignon. Impact de L'urbanisation Sur la Nappe Alluviale Au Confluent Rhône - Durance." *Géologues* N°167: 61–64.

Nofal, S., Y. Travi, A.-L. Cognard-Plancq, and V. Marc. 2019. "Impact of Infiltrating Irrigation and Surface Water on a Mediterranean Alluvial Aquifer in France Using Stable Isotopes and Hydrochemistry, in the Context of Urbanization and Climate Change." *Hydrogeology Journal* 27: 2211–2229. https://doi.org/10.1007/s10040-019-01989-y.

Olioso, A., R. Lecerf, A. Baillieux, et al. 2013. "Modelling of Drainage and Hay Production Over the Crau Aquifer for Analysing Impact of Global Change on Aquifer Recharge." *Procedia Environmental Sciences* 19: 691–700. https://doi.org/10.1016/j.proenv.2013.06.078.

Poulain, A., V. Marc, M. Gillon, et al. 2021. "Multi Frequency Isotopes Survey to Improve Transit Time Estimation in a Situation of River-Aquifer Interaction." *Watermark* 13: 2695. https://doi.org/10.3390/w13192695.

Racz, A. J., A. T. Fisher, C. M. Schmidt, B. S. Lockwood, and M. L. Huertos. 2012. "Spatial and Temporal Infiltration Dynamics During Managed Aquifer Recharge." *Groundwater* 50: 562–570. https://doi.org/10.1111/j.1745-6584.2011.00875.x.

Reszler, C., and J. Fank. 2016. "Unsaturated Zone Flow and Solute Transport Modelling With MIKE SHE: Model Test and Parameter Sensitivity Analysis Using Lysimeter Data." *Environment and Earth Science* 75: 253. https://doi.org/10.1007/s12665-015-4881-x.

Sasidharan, S., S. A. Bradford, J. Šimůnek, and S. R. Kraemer. 2021. "Comparison of Recharge From Drywells and Infiltration Basins: A Modeling Study." *Journal of Hydrology* 594: 125720. https://doi.org/10.1016/j.jhydrol.2020.125720.

Scanlon, B. R., R. W. Healy, and P. G. Cook. 2002. "Choosing Appropriate Techniques for Quantifying Groundwater Recharge." *Hydrogeology Journal* 10: 18–39. https://doi.org/10.1007/s10040-001-0176-2.

Schubert, M., M. Lin, J. F. Clark, et al. 2024. "Short-Lived Natural Radionuclides as Tracers in Hydrogeological Studies – A Review." *Science of the Total Environment* 920: 170800. https://doi.org/10.1016/j.scitotenv.2024.170800.

Séraphin, P., C. Vallet-Coulomb, and J. Gonçalvès. 2016. "Partitioning Groundwater Recharge Between Rainfall Infiltration and Irrigation Return Flow Using Stable Isotopes: The Crau Aquifer." *Journal of Hydrology* 542: 241–253. https://doi.org/10.1016/j.jhydrol.2016.09.005.

Sivakumar, M. 2021. "Climate Change, Agriculture Adaptation, and Sustainability." In *Climate Resilience and Environmental Sustainability Approaches: Global Lessons and Local Challenges*, edited by A. Kaushik, C. P. Kaushik, and S. D. Attri, 87–109. Singapore: Springer. https://doi.org/10.1007/978-981-16-0902-2_6.

Sobaga, A., F. Habets, N. Beaudoin, J. Léonard, and B. Decharme. 2024. "Decreasing Trend of Groundwater Recharge With Limited Impact of Intense Precipitation: Evidence From Long-Term Lysimeter Data." *Journal of Hydrology* 637: 131340. https://doi.org/10.1016/j.jhydrol.2024.131340.

Stumpp, C., P. Maloszewski, W. Stichler, and J. Fank. 2009. "Environmental Isotope (δ18O) and Hydrological Data to Assess Water Flow in Unsaturated Soils Planted With Different Crops: Case Study Lysimeter Station "Wagna" (Austria)." *Journal of Hydrology* 369: 198–208. https://doi.org/10.1016/j.jhydrol.2009.02.047.

Stumpp, C., W. Stichler, and P. Maloszewski. 2009. "Application of the Environmental Isotope δ18O to Study Water Flow in Unsaturated Soils Planted With Different Crops: Case Study of a Weighable Lysimeter From the Research Field in Neuherberg, Germany." *Journal of Hydrology* 368: 68–78. https://doi.org/10.1016/j.jhydrol.2009.01.027.

Tao, Z., H. Li, E. Neil, and B. Si. 2021. "Groundwater Recharge in Hillslopes on the Chinese Loess Plateau." *Journal of Hydrology: Regional Studies* 36: 100840. https://doi.org/10.1016/j.ejrh.2021.100840.

Tebaldi, C., K. Hayhoe, J. M. Arblaster, and G. A. Meehl. 2006. "Going to the Extremes." *Climatic Change* 79: 185–211. https://doi.org/10.1007/s10584-006-9051-4.

Tweed, S., N. Munksgaard, V. Marc, et al. 2016. "Continuous Monitoring of Stream δ18O and δ2H and Stormflow Hydrograph Separation Using Laser Spectrometry in an Agricultural Catchment." *Hydrological Processes* 30: 648–660.

United Nations. 2018. *Sustainable Development Goal 6 Synthesis Report 2018 on Water and Sanitation*. United Nations publisher, New York, NY: United Nation. ISBN: 978-92-1-101370-2.

van Wyk, Y., M. A. Dippenaar, and E. Ubomba-Jaswa. 2024. "Enhancing Hydrological Analysis by Incorporating Environmental and Artificial Tracers of an Altered Vadose Zone: A Systematic Review." *Journal of African Earth Sciences* 212: 105209. https://doi.org/10.1016/j.jafrearsci.2024.105209.

Weiler, M. 2017. "Macropores and Preferential Flow—A Love-Hate Relationship." *Hydrological Processes* 31: 15–19. https://doi.org/10.1002/hyp.11074.

Wiekenkamp, I., J. A. Huisman, H. R. Bogena, H. S. Lin, and H. Vereecken. 2016. "Spatial and Temporal Occurrence of Preferential Flow in a Forested Headwater Catchment." *Journal of Hydrology* 534: 139–149. https://doi.org/10.1016/j.jhydrol.2015.12.050.

Zhang, J., T. Lei, L. Qu, et al. 2017. "Method to Measure Soil Matrix Infiltration in Forest Soil." *Journal of Hydrology* 552: 241–248. https://doi.org/10.1016/j.jhydrol.2017.06.032.

Zhang, X., N. Wang, L. Cao, et al. 2024. "Analysis of the Contribution of Rainfall to Recharge in the Mu Us Desert (China) Based on Lysimeter Data." *Hydrogeology Journal* 32: 279–288. https://doi.org/10.1007/s10040-023-02750-2.

Zouari, K., R. Trabelsi, L. L. Araguás Araguás, S. Hussaini, S. Rabe, and A. Alassane. 2024. "Use of Hydrochemical and Isotopic Tracers to Investigate the Groundwater Quality and Recharge Processes of the Shared Iullemeden Aquifer System in the Sahel Region." *Hydrogeology Journal* 32: 219–240. https://doi.org/10.1007/s10040-023-02744-0.